AD-764 098

HIGH POWER DYE LASERS

A. R. Clobes, et al

United Aircraft Research Laboratories

Prepared for:

Advanced Research Projects Agency

30 July 1973

Security Classification

DOCUMENT CONTROL DATA - R&D

(Security classification of title, body of abstract and indexing annotation must be entered when the overall report is classified)

1 ORIGINATING ACTIVITY (Corporate author)	2a REPORT SECURITY CLASSIFICATION
UNITED AIRCRAFT RESEARCH LABORATORIES 400 MAIN STREET EAST HARTFORD, CONN. 06108	Unclassified
	2b GROUP

3 REPORT TITLE

HIGH POWER DYE LASERS

4 DESCRIPTIVE NOTES (Type of report and inclusive dates)

SEMI-ANNUAL TECHNICAL REPORT 1/1/73 - 6/30/73

5 AUTHOR(S) (Last name, first name, initial)

Clobes, A. R., Ferrar, C. M., Glenn, W. H., Ladd, G. O., Mack, M. E.

6 REPORT DATE	7a TOTAL NO OF PAGES	7b NO. OF REFS
7/30/73	58 57	42

8a CONTRACT OR GRANT NO. N00014-73-C-0284	9a ORIGINATOR'S REPORT NUMBER(S)
b PROJECT NO.	M921617-2
c	9b OTHER REPORT NO(S) (Any other numbers that may be assigned this report)
d	

10 AVAILABILITY/LIMITATION NOTICES

11 SUPPLEMENTARY NOTES	12 SPONSORING MILITARY ACTIVITY
	ARPA

13 ABSTRACT

This report describes the design, construction and testing of a high power, repetitively pulsed, flashlamp pumped dye laser. To date an average power of 10 watts has been obtained.

DDC
AUG 6 1973
C

DISTRIBUTION STATEMENT A
Approved for public release;
Distribution Unlimited

DD FORM 1473
1 JAN 64

Security Classification

UNITED AIRCRAFT CORPORATION
RESEARCH LABORATORIES

Report Number: M-921617-2
Semi-Annual Technical Report for the period
1 January 1973 to 30 June 1973

HIGH POWER DYE LASERS

ARPA Order No.   1806 AMEND #9/11-15-72
Program Code: 3E90
Contractor: United Aircraft Research Laboratories
Effective Date of Contract: 1 January 1973
Contract Expiration Date: 28 February 1974
Amount of Contract: $149,638.00
Contract Number: N00014-73-C-0284
Principal Investigator   Dr. William H. Glenn (203) 565-5411
Scientific Officer: Director, Physics Programs ONR
Short Title: High Power Dye Lasers
Reported By: G. O. Ladd, M. E. Mack, A. R. Clobes,
                                        W. H. Glenn, and C. M. Ferrar

The views and conclusions contained in this document are those of the
author and should not be interpreted as necessarily representing the official
policies, either expressed or implied, of the Advanced Research Projects
Agency or the U. S. Government.

Sponsored By
Advanced Research Projects Agency
ARPA Order No. 1806

UNITED AIRCRAFT RESEARCH LABORATORIES
SEMI-ANNUAL REPORT M921617-2
FOR THE PERIOD 1 JANUARY 1973 - 30 JUNE 1973

TECHNICAL REPORT SUMMARY

Prior to the start of this contract, UARL had developed a highly reliable, long life flashlamp for dye laser pumping. This lamp is an unconfined arc, i.e. a long spark gap. The position of the arc is stabilized by a vortex flow of the working gas. The gas used is argon with an admixture of CO_2 to control the breakdown voltage. This lamp was used in a specially designed pumping cavity to pump a Rhodamine 6G dye laser. An average power of 2 watts was achieved, nominally at 10 pps, 0.2 joules per pulse and with a pulse duration of approximately 1 microsecond. The goal of this contract is to scale this laser up to a higher average power with a design goal of 50 watts. An additional goal is to investigate techniques for rapidly tuning the output of the laser during a single pulse. Subsequent signal processing of such a frequency swept pulse would allow a time resolution much shorter than the total pulse duration if the laser were used in a ranging application.

Under this contract, a higher power dye laser has been designed and fabricated. At the present time this laser has produced an average power of 10 watts, at a repetition rate of 20 pps and an energy per pulse of 0.5 joules. This is the highest average power that has been reported to date for a repetitively pulsed dye laser. This performance was limited by the 9 KVA that was available from the power supply that was used for the test, i.e. the repetition rate was limited by the maximum available current. A company owned power supply having a 64 KVA capacity has recently been installed and will be used to test the limits of the present laser configuration.

The present flashlamp uses argon as the working gas. Commercial flashlamps use xenon because it is found to give a higher efficiency of conversion from electrical input to optical output. In some cases almost an order of magnitude increase in the output in the useful wavelength region is observed. If a substantial increase in the efficiency of the UARL flashlamp could be achieved, much higher laser output could be achieved. Tests are presently underway to compare the efficiencies of argon and xenon. One disadvantage of xenon is its cost. The use of xenon in the flowing lamp would require a closed cycle flow; the cost of an open cycle would be prohibitive.

Several techniques have been considered for the rapid frequency tuning of the dye laser including mechanical, electro optic, acoustooptic techniques as well as an acoustically driven, resonant Fabry Perot filter. The last technique appears to be the most promising. Components have been ordered for experiments on frequency sweeping that will be carried out during the next reporting period.

1

HIGH POWER DYE LASER

Introduction

To achieve the high average power output from a dye laser that is the goal of this contract, a careful design of the flashlamp, dye cell, pumping cavity, electrical excitation scheme, gas and liquid handling systems is required. The flashlamp that was chosen was the vortex stabilized, unconfined arc lamp. This lamp was developed at UARL prior to the start of work on this contract and was used to pump a moderate power dye laser with an output of 2 watts. The major part of the effort to date on this contract has involved the scaling up of this type of laser to higher power levels. To date, 10 watts of average power have been obtained, and this power level was limited not by the laser but by the available power supply. The following sections describe the design considerations, construction and testing of the high average power dye laser and discuss the steps that will be taken to achieve still higher power operation.

Flashlamp Design

The flashlamp that is being used is an unconfined arc, i.e. a long spark gap. This flashlamp has been operated at an input energy of up to 250 joules per pulse and at a repetition rate of up to 20 pps. The lamp has a conversion efficiency of 13 - 17%, depending on the input energy. It produces pulses of 1 - 2 microseconds duration. The lamp incorporates a vortex gas flow scheme in which the working gas is introduced tangentially at the envelope wall and subsequently swirls inward and exits through the electrodes. This gas flow serves two purposes. It stabilizes the position of the arc by creating a maximum E/P ratio in the axis of the lamp, thus preventing arc wander. In addition, the gas flow cools the lamp structure and sweeps away any of the products that might be sputtered off the electrodes. This prevents contamination and results in an exceptionally long lifetime, in excess of 2×10^5 shots. The lifetime is limited by the formation of color centers in the quartz envelope and could be extended by the use of UV grade quartz. A detailed discussion of the operation of the lamp is presented in Appendix I of this report. This appendix represents a portion of a paper entitled, "Vortex Stabilized Flashlamps for Dye Laser Pumping" by M. E. Mack that is being prepared for publication.

Cavity Design

To maintain arc stability vortex stabilized flashlamps require an axially symmetric electrical environment. As a consequence of this requirement many of the

2

commonly used pumping cavities, including the cylindrical ellipse and the close coupled pumping geometry, cannot be used with this type of lamp. Fortunately, there does exist a class of efficient pumping cavities, including some of the more commonly used exfocal cavities, which is ideally suited for present purposes. These cavities consist of some appropriate figure of revolution with the lamp and the laser medium positioned coaxially along the revolution axis of the cavity. The most frequently used of such cavities is the exfocal elliptical pumping cavity.

As the name suggests the exfocal elliptical pumping cavity is an ellipse of revolution, in this case with the major axis as the axis of rotation. The lamp and the laser are both located on the major axis with the lamp positioned between one focus and the corresponding vertex and, the laser material, between the other focus, and its vertex. The exfocal elliptical pumping cavity was first introduced in the early 1960's for pumping ruby lasers (Ref. 1). It is presently used in a series of solid state commercial laser systems marketed by Siemens Corporation. The threshold and output obtained with these commercial systems rival the best obtainable with elliptical cylinder pumping geometries. An excellent treatment of the imaging properties of the exfocal elliptical cavity is to be found in a recent paper by Mahlein and Zeidler (Ref. 2).

Although not technically an exfocal cavity the cavity devised recently by Danielmeyer and Barro (Ref. 3) falls in the general class of cavities delineated above. This cavity consists of a cylinder with conical pieces attached at each end. The lamp is mounted in one of these conical end pieces, while the laser rod is mounted in the other. The chief virtue of this unusual cavity is its excellent imaging properties. However, the arrangement has one serious drawback, and that is, that much of the light leaving the lamp and striking the conical end wall, is reflected back into the lamp housing. As a consequence the efficiency of this cavity would be relatively low.

For pumping dye lasers, we have used an exfocal spherical cavity. This configuration offers nearly all the advantages of the exfocal elliptical cavity and is more easily and less expensively fabricated. The arrangement of the flashlamp and the dye cell in the pump cavity is shown in Fig. 1. The lamp and cavity are shown here mounted on a coaxial capacitor as was used in the earlier, lower power lamp. The actual pumping cavity consists of two spun aluminum hemispheres, which snap together. To achieve a high reflectance surface on the hemispheres, the metal spinnings were Kanogen (electrodeless nickel) plated, the plating was polished on the interior surfaces and aluminum was then evaporated on the plating. This procedure gives the necessary high reflectance (to 90% depending on the care taken to polish the Kanogen), in a cavity, which can be easily drilled or machined and, which can be readily water cooled as the need arises.

The lamp housing is located in the lower hemisphere. The positioning of the arc along the axis of the hemisphere is discussed below. The dye laser dye cell is located in the upper hemisphere. A spiderlike arrangement of four thin walled stainless steel tubes supports the interior end of the dye cell and also provides

3

a channel for liquid flow. The optical cavity for the laser is formed by a high reflectance mirror (> 99%) attached to the interior end of the dye cell and by a changeable external mirror. The cavity length can be varied down to a minimum of about 11 cm.

The position of the arc along the axis of the lower hemisphere and the length of the arc are instrumental in determining the intensity distribution along the axis in the upper hemisphere (i.e., within the dye cell). These factors also affect the escape efficiency from the lamp housing; that is, the fraction of the light emitted by the lamp which is not blocked by the electrodes and electrode supports. To investigate these effects more quantitatively a computer simulation of the cavity has been carried out. The arc of the flashlamp was divided into a number of equal segments (usually 20). From the center of each segment a bundle of rays with one ray every $0.5°$ was emitted with a Lambertian intensity distribution. The axis of the upper hemisphere was then divided into segments (again usually 20) and the number of ray crossings in each segment were recorded by the computer. The rays were weighted according to the initial intensity and according to sphere reflectivity and the number of reflections made. In this way it was possible to determine lamp escape efficiency, overall cavity efficiency and axial pumping uniformity. In regard to pumping uniformity it should be noted that because of the axial symmetry of the cavity, the radial pumping distribution is perfectly symmetrical. This is of great value in minimizing thermal effects due to pumping in the dye solution.

Figure 2 shows some of the computer solutions obtained for various positions of a 1.5 cm arc along the lower half axis of an 8" diameter sphere. In practice the arc position is varied by changing the lengths of the two electrodes within the lamp housing (see Fig. 3). The total variation in arc position possible is restricted by the fixed lamp end support pieces. In Fig. 2 the arc position x, and the image position, x', are measured from the center of the sphere and are normalized by the sphere radius, a. (Here a=4" corresponds to the 1.5 cm arc length.) In all the cases shown in Fig. 2 the sphere reflectivity was taken to be R = 0.9. Fig. 2 also gives the total illuminating efficiency, ϵ_T, for the particular lamp arrangement, as well as an axial intensity uniformity factor, η. The total illuminating efficiency, ϵ_T, is defined here as the ratio of the total power in the image to the total power radiated by the arc as modeled by the ray tracing scheme. The efficiency, ϵ_L, includes, therefore, the lamp escape efficiency, ϵ_L, which can be obtained from the computer program by setting R=1. The axial intensity uniformity factor, η, is defined as the integral under the relative intensity curve (Fig. 2) divided by the total length of the image. A perfectly uniform intensity distribution would give $\eta = 1$.

For the 1.5 cm arc the optimum position in terms of efficiency and uniformity is for $0.40 \leq x/a \leq 0.55$; that is, for $1.6" \leq x \leq 2.2"$. The ray tracing in Fig. 3 is constructed for this case. The optimum illuminating efficiency for the 1.5 cm arc

4

is $\epsilon_T = 72\%$ and the uniformity is $\eta = 73\%$. The lamp escape efficiency with this arrangement is $\epsilon_L = 82\%$, so that most of the light loss is due to blockage by the lamp housing rather than to actual losses in the cavity. In fact, from the sphere reflectivity, the total efficiency and the lamp escape efficiency, we can define an effective number of reflections, N, such that $R^N = \epsilon_T/\epsilon_L$. For this case, $N = 1.37$. The ray tracing, Fig. 3, also confirms that most of the rays suffer only one reflection. From this ray tracing one might expect a substantially lower lamp escape efficiency than the 82% calculated. However, it must be remembered that the light leaving the arc has a Lambertian angular intensity distribution. Consequently, the light blocked by the end supports accounts for a smaller fraction of the light than would be the case, if the radiation pattern were isotropic. In any case the pumping efficiency is quite good.

The axial pumping uniformity is also good, especially considering that the dye cells used are often frosted on the outside. Moreover, as noted above, the axial intensity distribution is not as critical as the radial distribution in determining thermal distortion. Here, of course, the radial distribution is completely symmetric.

Finally, it should be observed that the "image" is substantially lengthened in comparison to the arc. In this case, the increase is approximately 5 fold. If desired, much higher lengthening factors are possible.

Figure 4 shows the result for a 6 cm long arc. In this case, the arc and the "image" are about the same length. This is also the maximum length arc that can be accomodated in the present lamp housing. Here the lamp escape efficiency is $\epsilon_L = 78\%$. With a 90% sphere reflectivity, the total illuminating efficiency is $\epsilon_T = 67\%$ corresponding to an effective number of reflections of $N = 1.53$. The axial uniformity is also good with $\eta = 72\%$. Although the total illuminating efficiency in this case is slightly less than with the shorter arc, it must be borne in mind that the longer arc, itself, will be more efficient than the shorter arc.

The computations outlined above serve to illustrate the efficiency and flexibility of the exfocal spherical pumping cavity. These computations do omit two factors generally of some importance, namely, the finite diameter of the lamp arc and the dye cell, and, multiple passes through the pumping cavity. In this case the latter factor is negligible, since with the dye concentrations normally used, only a few percent of the incident pump light will pass through the dye cell. A 2×10^{-4} M solution of Rhodamine 6G in ethanol, for example, has an optical density, D, of $D \geq 2$ over the spectral range from 2000 to 5000 Å. Because of the moderately high color temperature of the lamp, this includes nearly all of the lamp emission.

Experimentally, the diameter of the "image" in the upper hemisphere is roughly the same as that of the arc. Since the arc diameter is generally smaller than the dye cells used, the pumping density in the dye is determined by the diameter, and therefore, the volume of the dye cell. Of course, the dye concentration must be adjusted to assure that all the pump light is absorbed. For dyes with a high threshold, a relatively small dye cell diameter should be used. On the other hand, in dyes

with a low threshold, a larger dye cell diameter may be advantageous. In the
present arangement varying the dye cell diameter and consequently, the pumping
density, can be easily accomplished by the use of interchangeable dye cells with
various diameters. This added flexibility has already been used to an advantage.

Dye Laser Construction

As has been mentioned above, a vortex stabilized flashlamp and an exfocal
spherical cavity were used to produce an average power output of 2 watts prior
to the beginning of the present contract. This laser employed a 2 µfd, 25 Kv
low inductance coaxial capacitor that was connected to the flashlamp as shown
in Fig. 1. A photograph of this laser is shown in Fig. 5. This laser produced
an output pulse energy of 200 millijoules/pulse at a repetition rate of 10 pps.
An attempt to run this laser at a higher energy and a higher repetition rate
resulted in the failure of the energy storage capacitor due to overheating. A
number of attempts to achieve higher power output with rebuilt capacitors were
unseccessful. It was concluded that to meet the power and repetition rates pro-
posed for this contract, a different type of capacitor would be required. A
suitable capacitor was obtained from Tobe Deutschmann Laboratories. This capacitor
is physically much larger than the coaxial unit although its capacity is identical
(2 µfd). It is guaranteed for operation at 200 joules, 50 pps continuous operation.
The capacitor has a parallel plate output rather than a coaxial output. This
required a total redesign of the electrical transition between the capacitor and
the flashlamp. This, together with the redesign and construction of a higher
power flashlamp and dye laser head has represented the bulk of the work to date
on this contract.

Fig. 6 illustrates the high power laser that has been constructed under this
contract. The configuration is considerably different than that of the 2 watt
laser discussed above. The energy storage capacitor, the transition section, the
spherical laser pumping cavity, and the dye recirculation system may all be seen
in the Figure.

Figure 7 shows the construction of the transition section. It consists
basically of a parallel plate transmission line. The two aluminum plates are
separated by a plate of G-10 with a sheet of mylar on either side. The mylar
is necessary to prevent breakdown near the gap between the end of the insulator
on the capacitor and the G-10 plate. A hole is provided for the coaxial transition
section and the interior of the hole is lined with a ceramic tube. The aluminum
plates are tapered near the hole to eliminate the possibility of breakdown at
sharp curves. The entire transition assembly is bonded together with epoxy and
is bolted to the output terminals of the capacitor. The upper plate has provision
for water cooling.

6

The arrangement of the lamp is shown in a highly schematic form in Fig. 8. The gas enters the plenum at the bottom and passes through six tangential holes into the lamp itself. This tangential injection provides the vortex flow for arc stabilization. The gas swirls inward and exits through the electrodes with the major portion flowing out the anode, down the supporting tubing and out through the base plate. The base plate is cooled by thermal contact to the cooled aluminum plate. The upper portion of the assembly has separate provision for water cooling. Fig. 9 shows the anode assembly and Fig. 10 the cathode assembly which includes the vortex generator with input and output gas chambers, the ceramic insulator tube and the insulated lead for the trigger electrode. The pumping cavity is similar to that shown schematically in Fig. 1. Fig. 11 is a photograph of the top half of the pumping cavity. The dye cell is removed in this Figure. The dye cells are demountable and cells of different diameter may be installed as desired.

Figure 6 also illustrates the dye recirculation system. This consists of a stainless steel gear pump, a 5 micron in line millipore filter to remove particulate matter and cavitation bubbles two reservoirs having a total volume of 16 liters and the associated tubing and connectors. The dye reservoirs include a heat exchanger to maintain the dye solution at a constant temperature at high power levels of operation. The system can be degassed by means of an aspirator. It can be pressurized by means of an air driven bellows in one of the reservoirs, or it can be pressurized with any desired gas. The dye flow rate through the system is typically 3 gallons per minute or 0.2 liters/second. With a dye cell volume of approximately 10 cm^3, the dye is exchanged 20 times/second so that cumulative thermal effects can be eliminated at repetition rates up to 20 pps.

Dye Laser Performance

The performance of the dye laser was evaluated using two varieties of Rhodamine 6G commercial Rhodamine 6G chloride and specially purified Rhodamine 6G tetrafluoroborate in ethanol solutions. Both the dye concentrations and the output mirror reflectivity were optimized for maximum output. For both dyes the optimum concentration was found to be 1.5×10^{-4} M. and the optimum output reflectivity was about 35%. The results are shown in Fig. 12. In this figure the energy output is plotted as a function of the energy input for untuned, single shot operation. A maximum efficiency of 0.25% was achieved at a 100 joule input. With the Rhodamine 6G tetrafluoroborate the efficiency reached a maximum of 0.33% at 81 joules, and decreased to 0.25% at 200 joules. At 200 joules, the energy output was about 1/2 joule/pulse.

Figure 13 shows the power output as a function of repetition rate. For Rhodamine 6G chloride, an energy of 100 joules per pulse was used. At a repetition rate of 20 pps this gave an average power of 5 watts. The Rhodamine 6G tetrafluoroborate

7

was operated at an energy input of 200 joules per pulse and gave an average power of 10 watts. The power output at this point was limited by the available power supply. This power supply had a capacity of about 9 Kw. The flashlamp itself was only consuming 4 Kw (200 joules at 20 pps) but the remainder was dissipated in the ballast resistor in the capacitor charging circuit. The next step in the investigation will be to determine the limitation imposed by the laser in the output power. To accomplish this, a much larger power supply has been installed. This supply has a capacity of 64 Kw; it is shown in Fig. 14.

Future Plans

The first step that will be taken to achieve higher power levels of operation will be the operation of the dye laser with the new 64 Kw power supply discussed above. The power supply is presently installed and is being used to operate the laser at lower power levels. High power tests are awaiting the arrival of an additional energy storage capacitor to serve as a backup in the event of a catastrophic failure. The dye laser is being used for programs other than this contract and it is undesirable for it to have any extended down time. The new capacitor is expected to arrive in the near future.

The efficiency of the laser in its present form is limited to about 0.25%. This is a result of premature termination of the laser pulse due to thermal distortion. The distortion is caused by radial acoustic waves produced by the rapid heating of the dye solution during the pumping pulse. Theoretical modelling carried out in support of the experimental work has given good agreement with the experimental observations and has indicated that corrective measures may be possible. If self termination can be prevented, a two-to-three fold increase in laser efficiency and power output should be achievable.

The present flashlamp operates with argon as the working gas. Commercial wall stabilized lamps use xenon because of its higher electrical to optical energy conversion efficiency. If a comparable increase in efficiency of the vortex stabilized lamp could be realized, considerably higher output power could be obtained. Tests are underway to compare the relative efficiencies of argon and xenon. These are being carried out in a static (non flowing) lamp. In the absence of flow, the position of the arc is unstable but efficiency measurements may still be made. There is some preliminary indication that higher efficiencies may be obtained at low input energies in xenon but that the output shows saturation at the 200 joule input level. If these observations are confirmed, it would indicate that higher powers should be obtained by decreasing the energy input per pulse and increasing the repetition rate. This matter is presently under investigation.

FREQUENCY SWEEPING THE DYE LASER

Introduction

A variety of techniques have been developed for tuning the output of the dye laser. All of the techniques to date tune the laser from pulse to pulse for the case of flashlamp pumped lasers, or over a period of seconds or minutes for the laser pumped dye. The object of the work reported here is to sweep the laser frequency over a significant fraction of the available linewidth during one pulse which typically lasts 1 to 2 μsec. To date none of the available tuning techniques even approach the speed required and thus special techniques need to be developed. Some of the possible methods of fast sweep of the dye laser have been discussed and the limitations pointed out the proposal to the present contract (Ref. 4). One method of tuning a dye laser which has attracted much attention recently is the acousto-optic filter and its limitations to fast sweep are outlined in the following paragraphs. At present the most feasible method appears to be the resonant driven Fabry-Perot etalon and it is discussed below.

Acousto-Optic Filters

A dye laser tuning technique which has a potential for fast sweeping of the dye laser frequency, utilizes an acousto-optic filter. In this filter, an anisotropic crystal is oriented such that an incident optical signal of one polarization is diffracted into the orthogonal polarization by a collinearly propagating acoustic beam. For a given acoustic frequency, only a small range of optical frequencies will satisfy the $\vec{k}$ vector-matching condition, and only this small range of frequencies will be cumulatively diffracted into the orthogonal polarization. If the acoustic frequency is changed, the band of optical frequencies which the filter will pass is changed.

The acousto-optic filter technique of tuning a dye laser has been demonstrated by D. J. Taylor et. al. (Ref. 5). They used a Q-switched, frequency doubled Nd:YAG laser to pump a Rhodamine 6G dye laser. They were able to tune the dye laser output from 5445 Å to 6225 Å by varying the acoustic frequency from 58.2 to 45.0 MH$_z$. The tuning sensitivity of 59 Å/MH$_z$ would make this filter appear as an attractive candidate for fast frequency tuning of the flashlamp pumped dye laser. A problem arises due to the relatively slow acoustic velocity in the material. In one experiment a 3.5 cm long piece of Ca MoO$_4$ were used on the filter material. This material has an acoustic shear velocity of 3×10^5 cm/sec and thus it requires greater than 10 μsec for a change in acoustic frequency to propagate the length of the filter. Thus, any change in the acoustic frequency during the 1 to 2 μsec dye laser pulse would only have the effect of significantly widening the filter passband and it is doubtful that any frequency sweep would occur. The

problem could be circumvented to a certain extent by shortening the crystal length but this also reduces the interaction between the acoustic and optical beam, thus increasing the losses to the latter. Due to the relatively long interaction time required for proper functioning of the acousto-optic filter, it is doubtful that it will be useful in this program for fast frequency sweeping of the dye laser.

Resonant Driven Fabry-Perot Etalon

Relatively low finesse (20 to 30) etalons have been used to narrow the line-width of flashlamp - pumped dye lasers. The experimental results show that the laser linewidth can be narrowed to less than 1 $\overset{o}{A}$ by using two such etalons (Refs. 6, 7). Tuning of the laser output by tilting the etalons has also been demonstrated in previous experiments (Ref. 6). Due to obvious physical limitations, rapid tuning of the dye laser by tilting an intracavity etalon is not practical. Etalon tuning can also be done by varying the distance between the parallel reflecting surfaces which make up the etalon. Thermal tuning is much too slow. Another pos-sibility is to make the solid etalon from an electro-optic material. With a proper choice of crystal orientation and placement of electrodes, the distance between the parallel faces of the crystal could be made to increase or decrease by varying an applied electric field. This method of etalon tuning has a limitation which arises from the small thickness (a few mm or less) of the requisite etalon. Whether a transverse or a longitudinal field is applied to the thin etalon there is a problem of voltage breakdown from the use of a brittle material. The use of a solid etalon made from a piezoelectric material suffers from the same problems as an electrooptic material.

The problems of tuning a solid etalon can be circumvented by the use of an air etalon in which one mirror is fixed and a second paralled mirror is mounted to a piezoelectric tube. Commericially available scanning Fabry-Perots are made in this way. Mechanical displacement is achieved by piezoelectric expansion and contraction of the electrically driven tube. The difficulty of having to use very high voltages to obtain sufficiently large displacements can be overcome by driving the tube at its mechanical resonant frequency. For a given applied voltage, the resonant amplitude is larger than the static amplitude by a factor of Q which in general has values of 100 to 400. This technique has been used successfully to scan a free spectral range of 30 $\overset{o}{A}$ in 0.3 μsec with a finesse of 20 (Ref. 8). More recent re-sults by another group resulted in scanning a free spectral range of 23 $\overset{o}{A}$ in .5 μsec; a finesse of 13 and a peak applied voltage of 23 volts (Ref. 9). From the results reported in the literature it appears possible to scan an etalon by 10's of $\overset{o}{A}$ in a fraction of a μsec using a resonant driven Fabry-Perot etalon. This appears to be the most feasible method of rapid tuning of the dye laser output and it is the method chosen for this program.
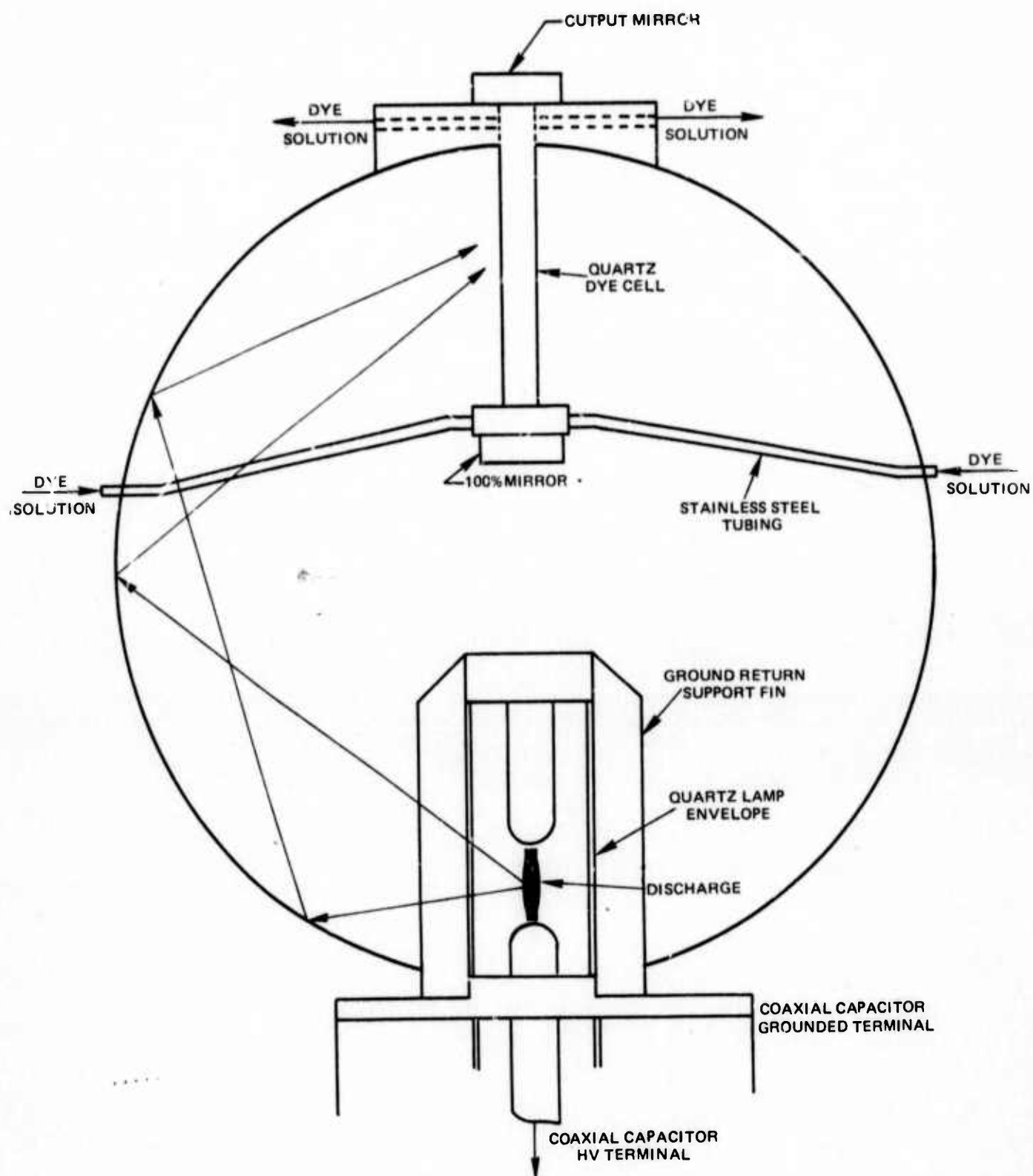
Thin walled cylindrical Pzt elements with a 1 inch O.D and length ranging from 1 inch to 4 inches have been ordered. The unloaded resonant frequency ranges from

15 to 60 KH$_z$. The piezoelectric material is lead zinconate titanate and it was chosen for its low loss tangent and high Q. The flat etalon mirrors have a λ/50 surface figure and coated for 90 percent reflectance at 5,900 Å. The theoretical etalon finesse using these mirrors is 30. We also have a pair of mirrors with the same specifications except they are coated for 6328 Å and will be used external to a He:Ne laser to check out the free spectral range, scan rate and the finesse of the etalon. Assuming that the etalon checks out satisfactorily, the mirrors will be replaced with those coated for 5,900 Å and the assembly placed intracavity to the dye laser.

Although the resonant driven Fabry-Perot etalon is conceptually very simple an anticipated problem arises from heating of the Pzt element due to the finite loss tangent of the material. Such heating could make it very difficult to hold the two etalon mirrors parallel. If a problem does arise, it can be circumvented to a certain extent by pulsing the electrical drive to the Pzt element.

REFERENCES

1. Roess, D.: Appl. Opt., $\underline{3}$, 259 (1964).

2. Mahlein, H. F., and G. Zeidler: Appl. Opt., $\underline{10}$, 872, (1971).

3. Danielmeyer, H. G., and J. M. Barro: to be published.

4. UARL Report P-L252; Sept. 1972.

5. D. J. Taylor et. al.; Appl. Phys. Letters vol. $\underline{19}$, p. 269, (1971).

6. M. E. Mack private communications.

7. G. M. Gale, Optics communications, $\underline{7}$, p. 86, (1973).

8. J. R. Greig and J. Cooper, Applied Optics, $\underline{7}$, p. 2166, (1968).

9. P. J. Brannon and F. M. Bacon, Applied Optics, $\underline{12}$, p. 142 (1973).

FIG. 1

M921617-2

CUTPUT MIRRCH

DYE SOLUTION

DYE SOLUTION

QUARTZ DYE CELL

DYE SOLUTION

100% MIRROR

STAINLESS STEEL TUBING

DYE SOLUTION

GROUND RETURN SUPPORT FIN

QUARTZ LAMP ENVELOPE

DISCHARGE

COAXIAL CAPACITOR GROUNDED TERMINAL

COAXIAL CAPACITOR HV TERMINAL

AXIAL INTENSITY DISTRIBUTION WITH A 1.5 cm ARC

FIG. 2

$0.30 \leq \frac{x}{a} \leq 0.45$

$R = 0.9$

$\epsilon_T = 0.67$

$\eta = 0.60$

$0.40 \leq \frac{x}{a} \leq 0.55$

$R = 0.9$

$\epsilon_T = 0.71$

$\eta = 0.73$

$0.60 \leq \frac{x}{a} \leq 0.75$

$R = 0.9$

$\epsilon_T = 0.71$

$\eta = 0.48$

$0.70 \leq \frac{x}{a} \leq 0.85$

$R = 0.9$

$\epsilon_T = 0.65$

$\eta = 0.43$

$\frac{x'}{a}$

FIG. 3
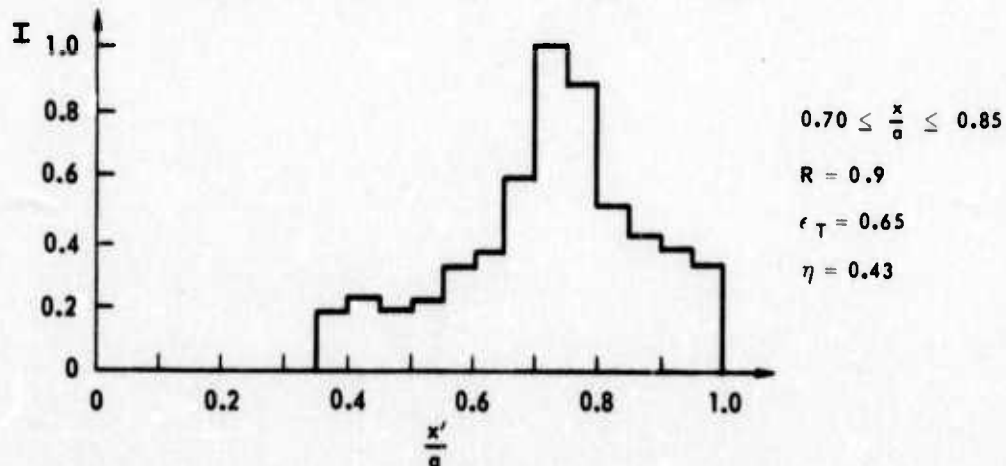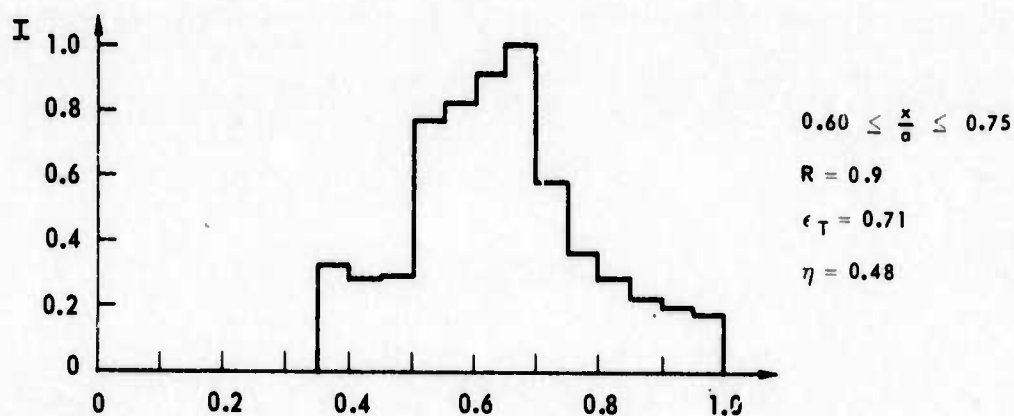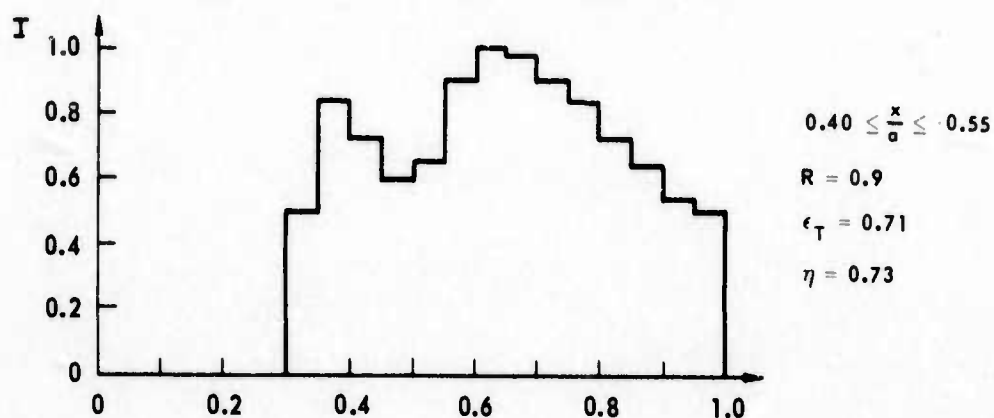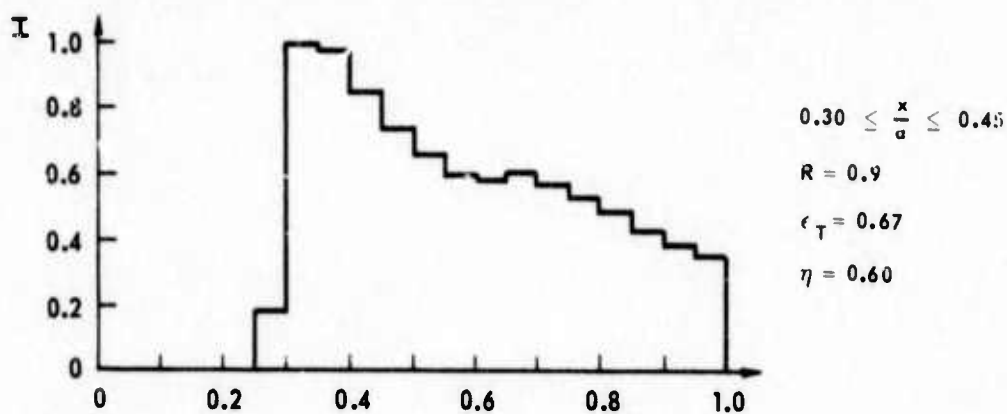
RAY TRACE – OPTIMALLY LOCATED 1.5 cm ARC

a = 4.0 in.
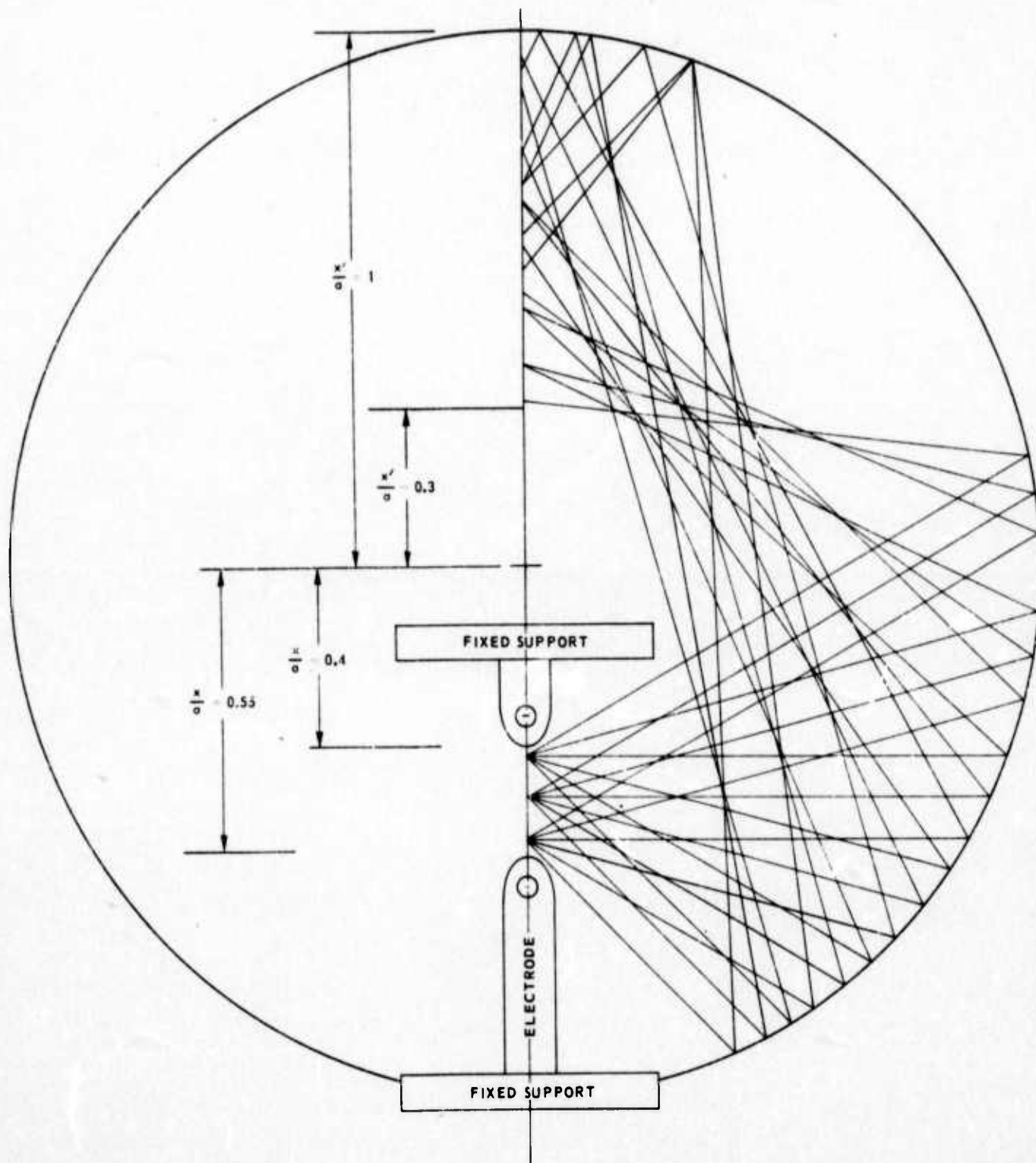
AXIAL INTENSITY DISTRIBUTION WITH A 6.0 cm ARC

FIG. 4

$0.3 \leq \dfrac{x}{a} \leq 0.9$

$R = 1.0$

$\epsilon_T = \epsilon_L = 0.78$

$\eta = 0.71$

$0.3 \leq \dfrac{x}{a} \leq 0.9$

$R = 0.9$

$\epsilon_T = 0.67$

$\eta = 0.72$

$0.3 \leq \dfrac{x}{a} \leq 0.9$

$R = 0.8$

$\epsilon_T = 0.56$

$\eta = 0.74$

$\dfrac{x^6}{a}$

16

FIG. 5

2 WATT DYE LASER

FIG. 6

HIGH POWER DYE LASER

FIG. 7
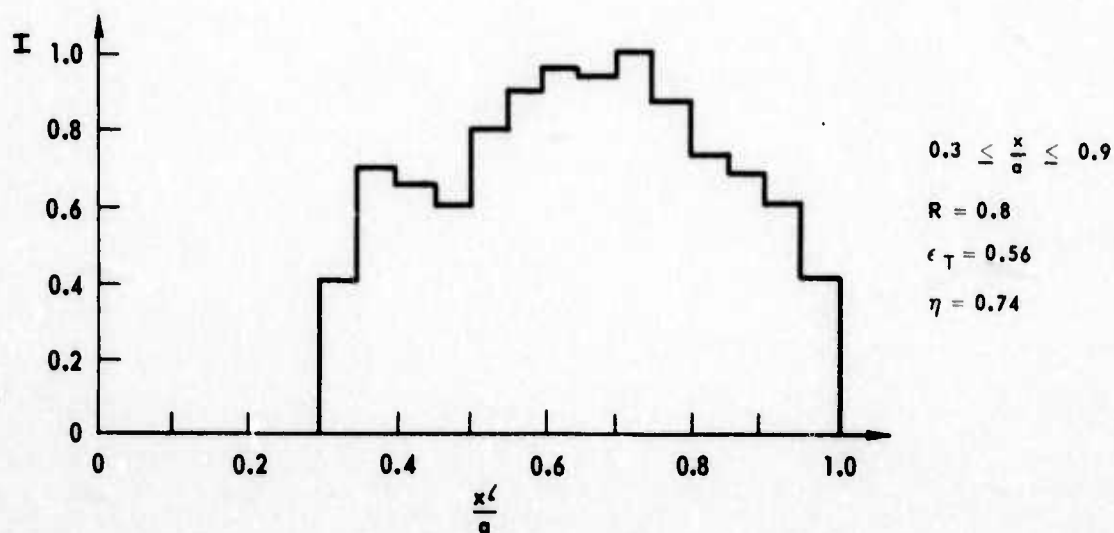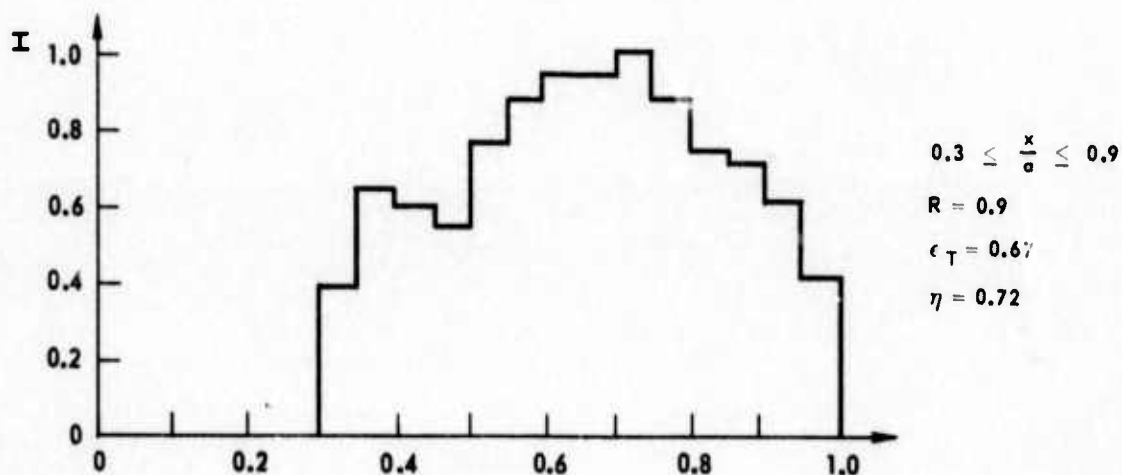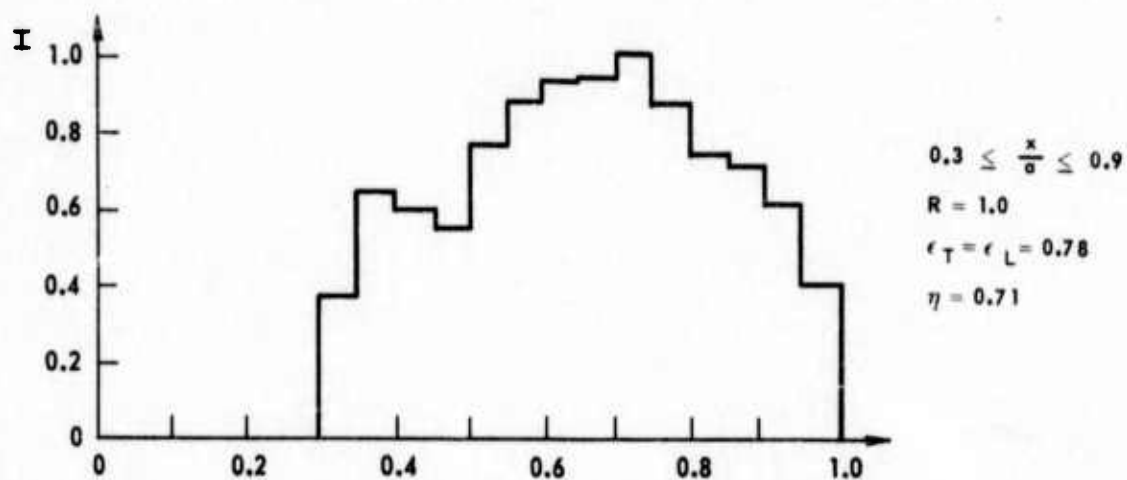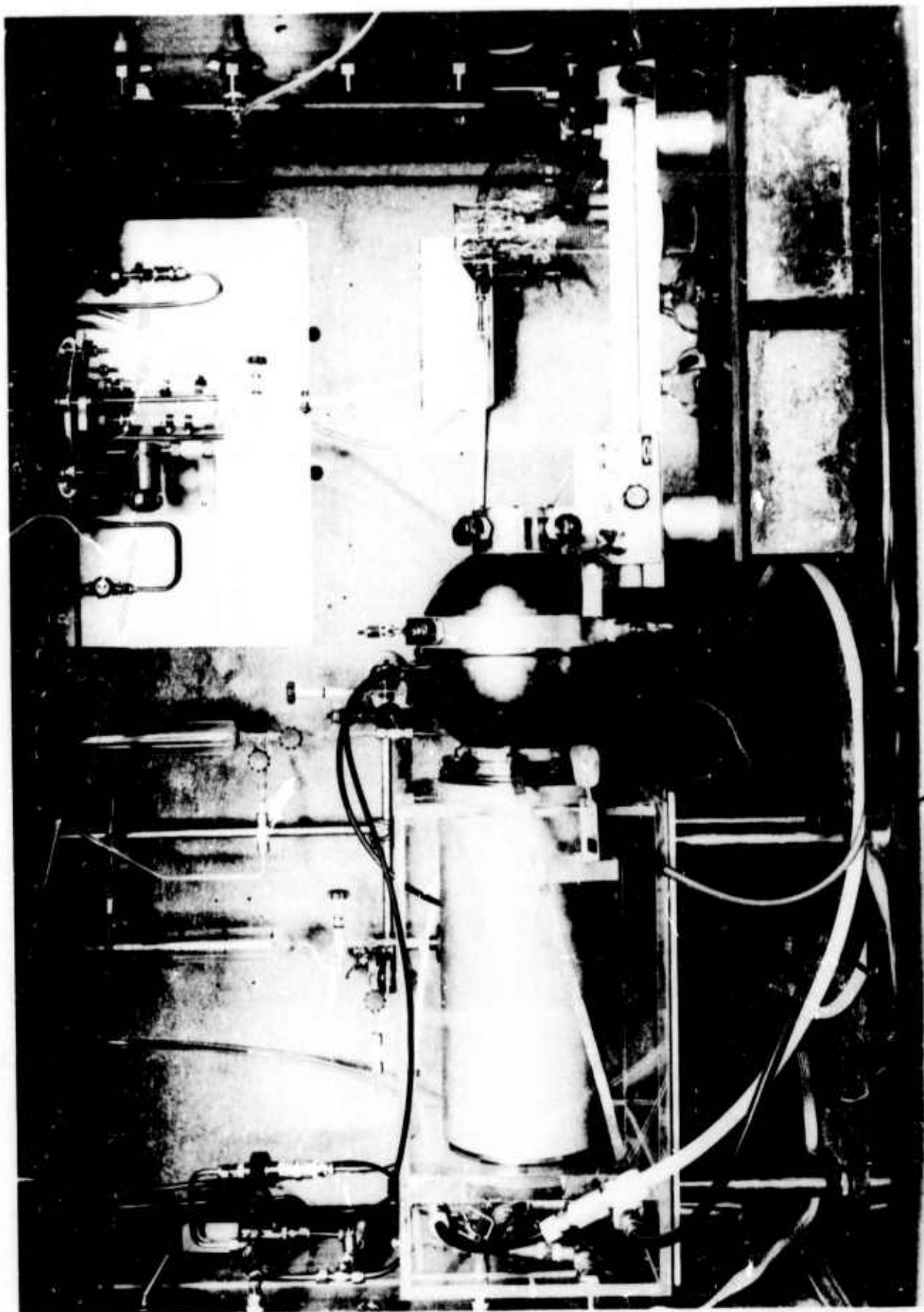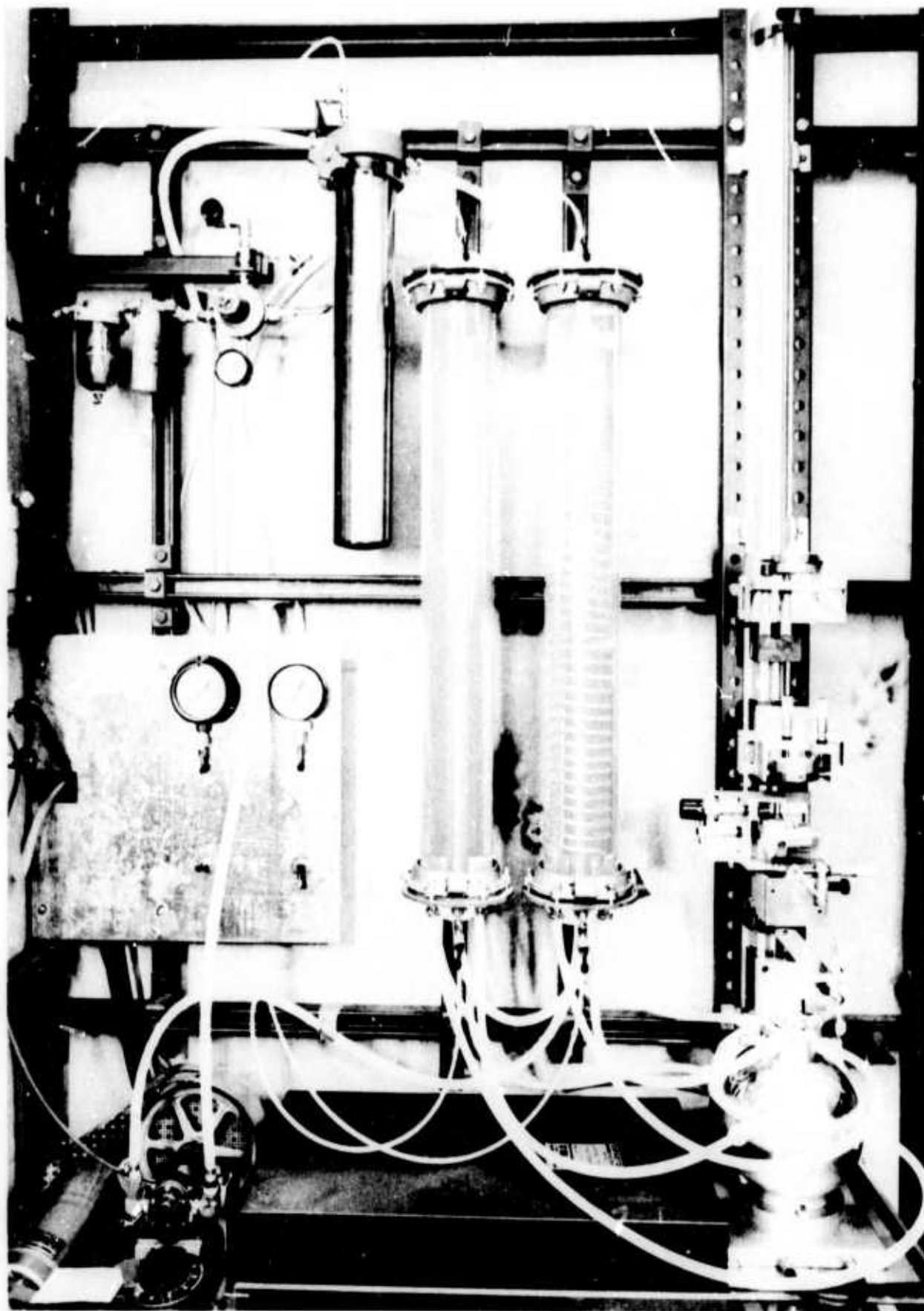
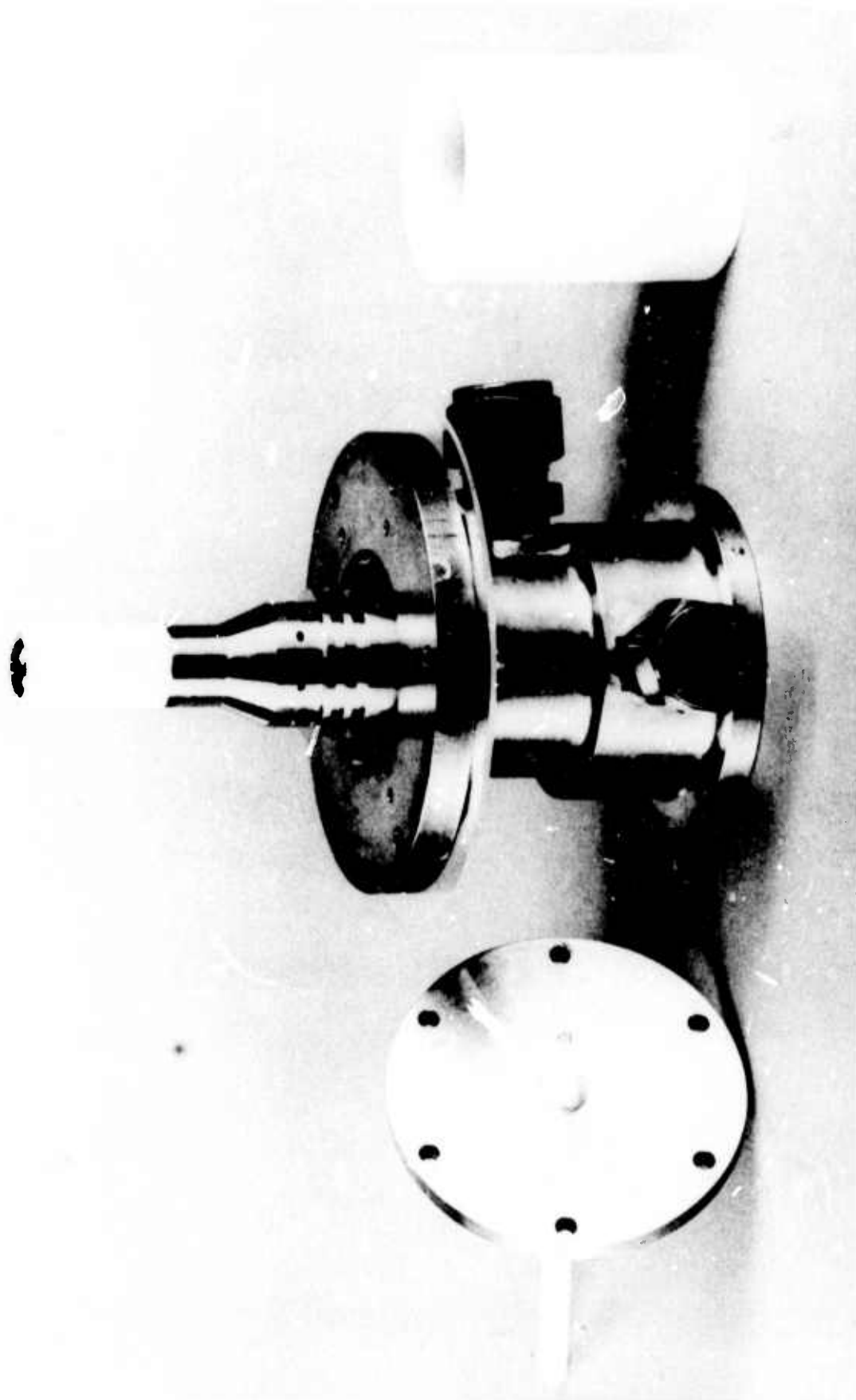SCHEMATIC DIAGRAM OF HIGH POWER LASER

TRANSTION SECTION
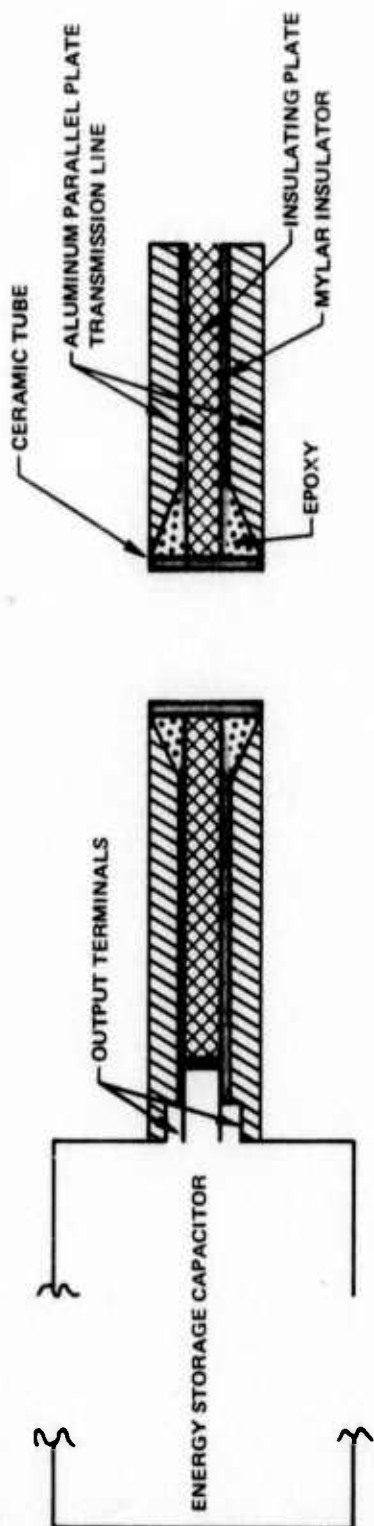
SCHEMATIC DIAGRAM OF FLASHLAMP
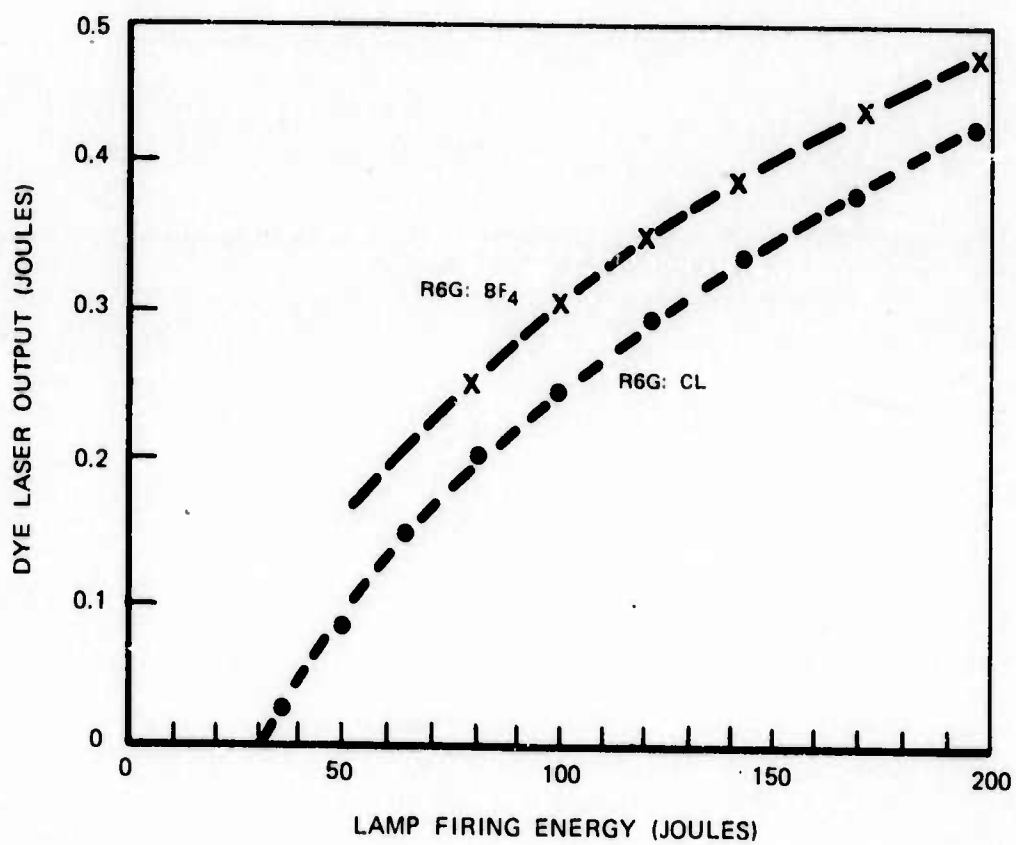ILLUSTRATING THE GAS FLOW PATH

TUBES TO SUPPORT ANODE
STRUCTURE AND PROVIDE
RETURN PATH FOR GAS

VORTEX GENERATORS

GAS OUT

TRANSITION SECTION

GAS IN

GAS OUT

TRIGGER ELECTRODE

ANODE ASSEMBLY

FIG. 10

CATHODE ASSEMBLY

FIG. 11
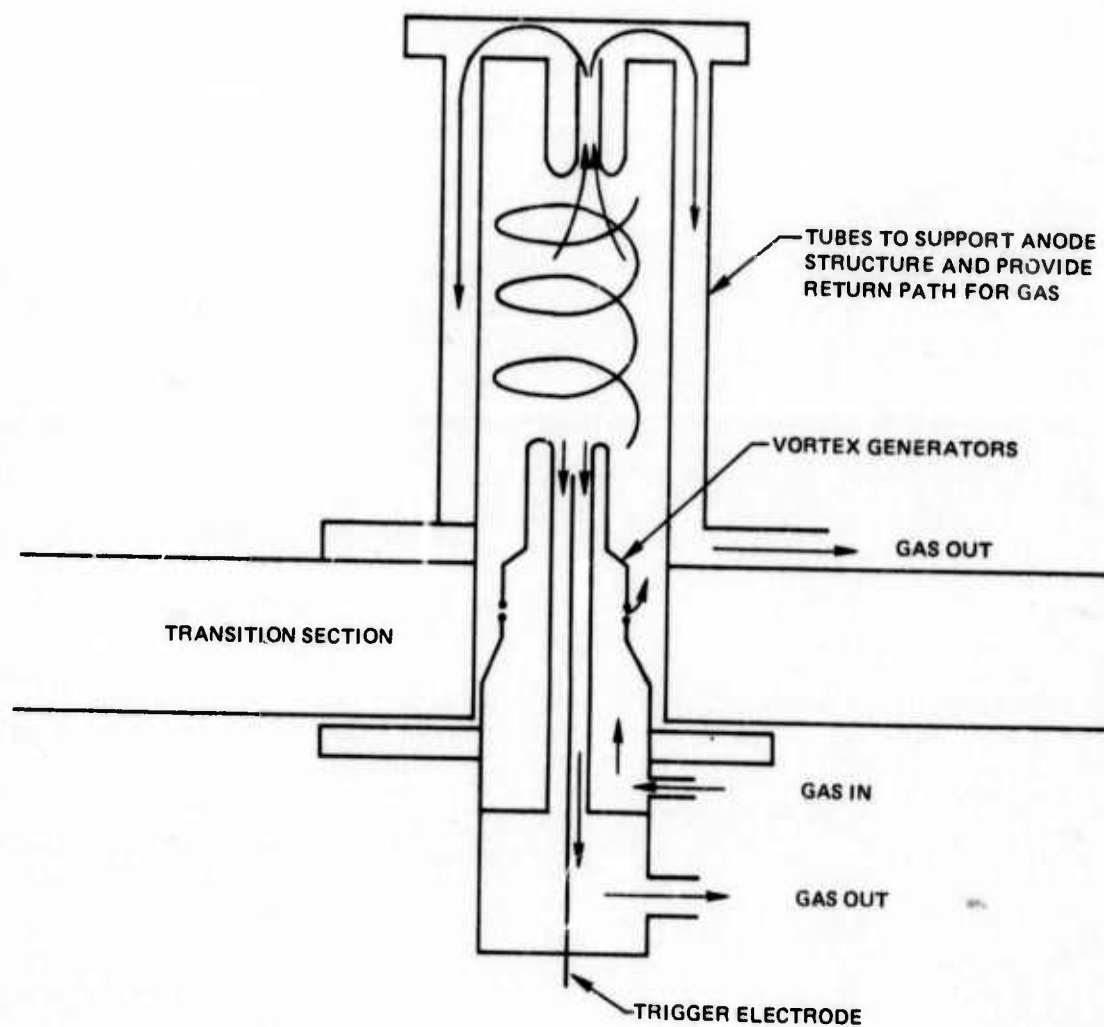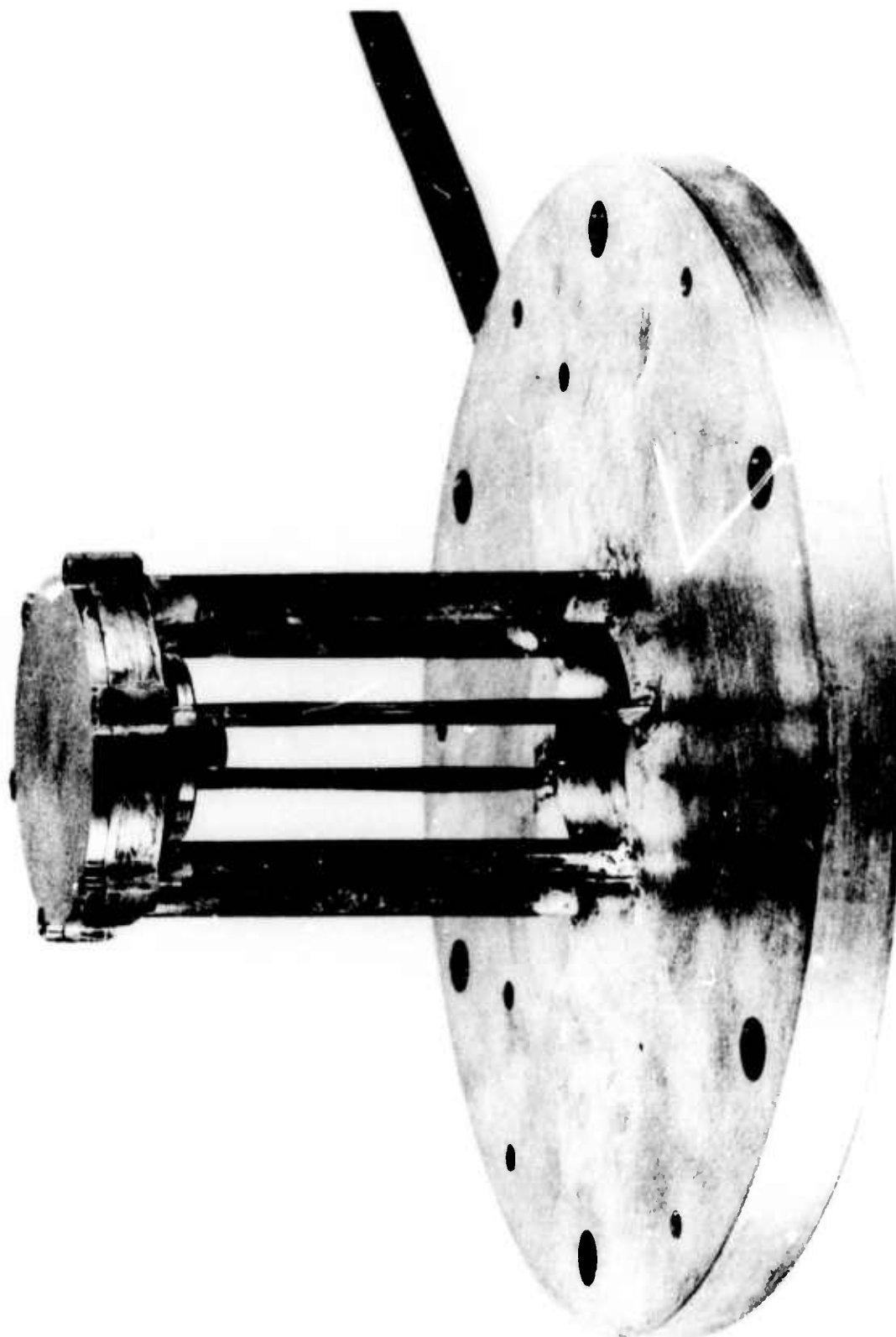
UPPER HEMISPHERE OF PUMPING CAVITY

FIG.12

DYE LASER ENERGY OUTPUT

$(1.5 \times 10^{-4}$ M RHODAMINE 6G IN ETHANOL R_1R_2 = 35%)

FIG. 13

DYE LASER POWER OUTPUT

64 KW POWER SUPPLY
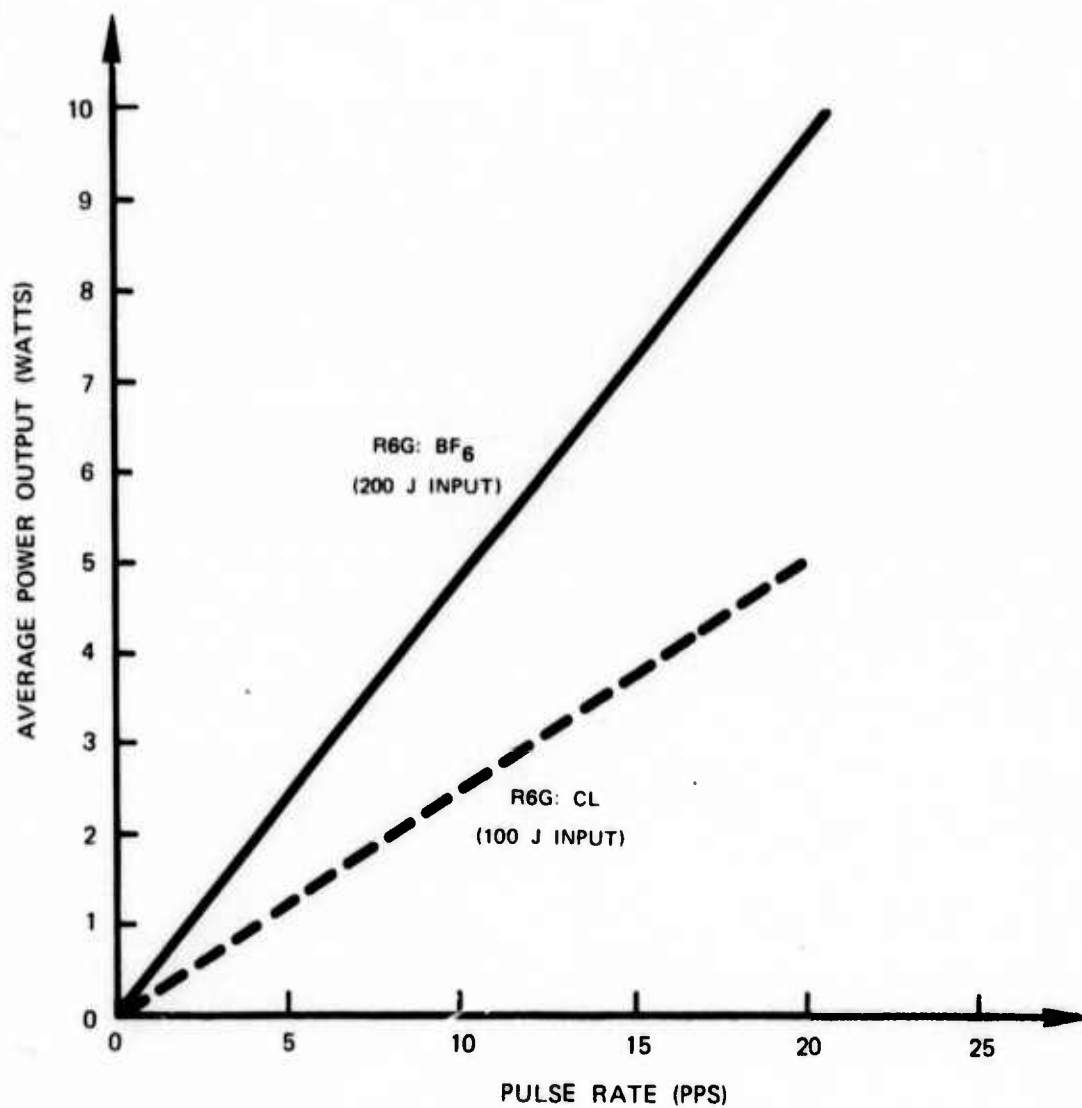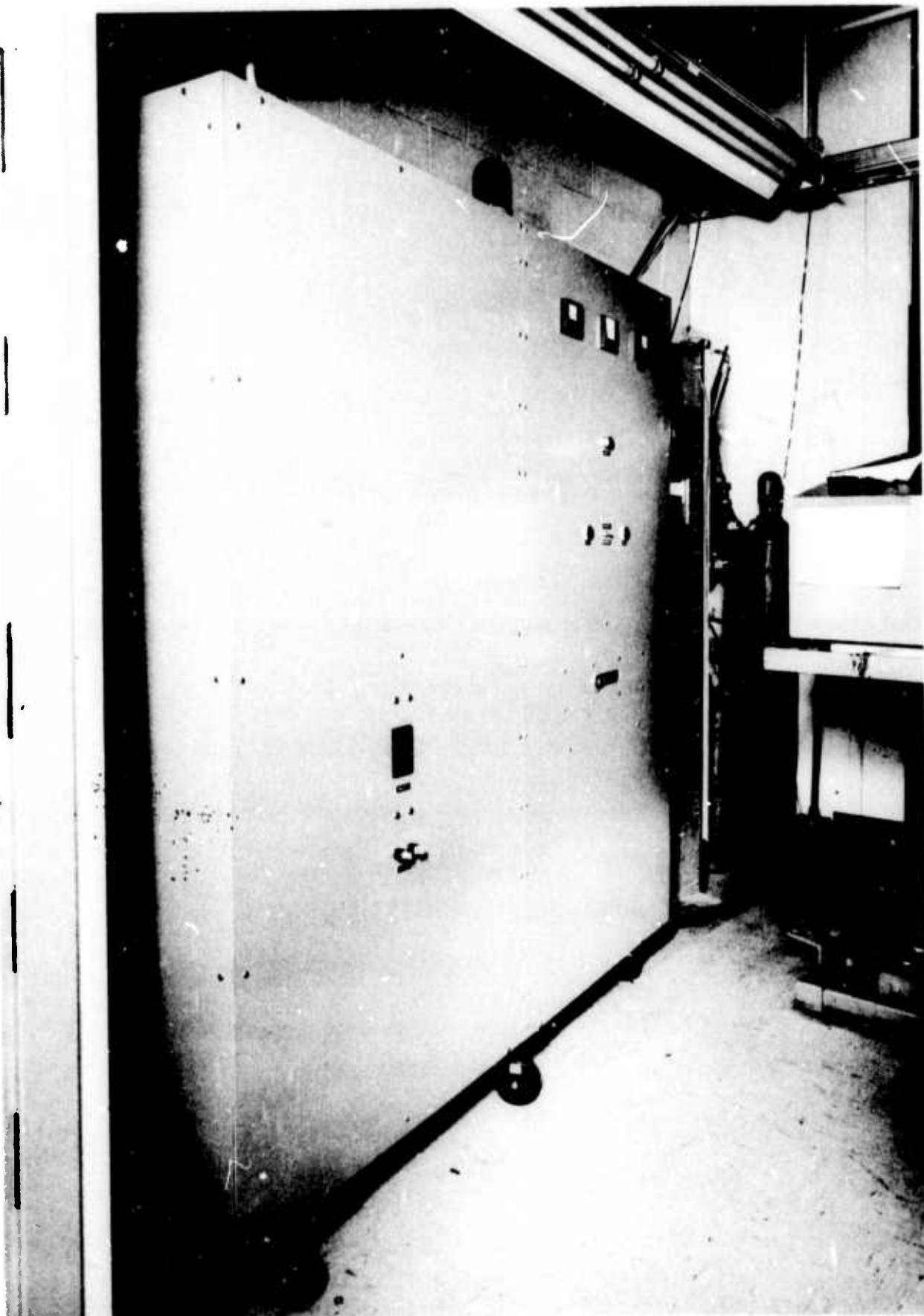
APPENDIX I

VORTEX STABILIZED FLASHLAMPS FOR DYE
LASER PUMPING

I. Introduction

In most of the dyes commonly used for dye lasers the fluorescent decay time
for the laser transition is in the range of from 2 to 10 nanoseconds. To overcome
such strong spontaneous emission losses and exceedingly intense pumping source is
required. The most practical way to achieve such power densities over volumes of
moderate extent is with a short duration pulsed flash. Initially, it was felt
that a fast risetime was also required to overcome losses due to the accumulation
of population in absorbing triplet states (Ref. 1, 2). More recently, a number of
chemical quenchers, including atmospheric oxygen, have been found, which effective-
ly deactivate the metastable triplets (Ref. 3-5). Nevertheless, the most success-
ful results in terms of power output and efficiency have been achieved with pumping
pulse durations in the 0.4 to 10 microsecond (μsec.) range (Ref. 6-11).

Flashlamps capable of handling a moderate ($\gtrsim$100J.) amount of energy with a
pulse duration of 10 μsec or less are constructed only with some difficulty. When
a flashlamp is fired, a shock wave is set up in the gas within the lamp. At any
given discharge duration, the shock wave intensity depends on the total energy
discharged. If the energy discharged exceeds the explosion limit for the lamp,
the shock wave developed will be sufficiently intense to rupture the lamp walls
and, consequently, destroy the lamp. Since the shock wave intensity increases
with decreasing pulse duration, the explosion limit for the lamp is correspondingly
reduced (Ref. 12). Catastrophic failure is often a major problem with fast rise-
time flashlamps.

Operated well below the explosion limit, flashlamp lifetime is then limited by
electrode erosion with the subsequent formation of opaque deposits on the lamp
jacket near the lamp electrodes and by wall vaporization in the hotter regions of
the discharge. Both electrode erosion and wall vaporization are accelerated by
the very high peak currents in the short duration flashlamps used for pumping dye
lasers. As a result the useful operating lifetime for these lamps is substantially
reduced in comparison to similar lamps operated in a long pulse (millisecond) mode.

Flashlamp pumped dye laser action was first demonstrated using the so-called
coaxial flashlamp. This device built by Sorokin et. al. (Ref. 2). was patterned
after the flash photolysis lamps of Claesson and Lindqvist (Ref. 13). The lamp
discharge takes place in the annular region between the dye cell, which forms the
inner wall of the lamp, and a cylindrical outer wall. The wall thickness of the
outer jacket can be made as thick as necessary to withstand the mechanical force
of the discharge. The inner wall is reinforced by the liquid within the dye cell.
Initially, these flashlamps were operated with air as the fill gas. More recently,

28

Furomoto and Ceccon demonstrated substantially improved operation using specially constructed coaxial tubes with xenon as the filling gas (Ref. 10, 14). Such flashlamps are now commercially available. A firing energy of 100 joules with a C.5 μsec duration is typical for the commercial units. At this firing energy the lifetime to half light output is of the order of 5000 shots.

Linear flashlamps are also widely used for pumping dye lasers. These lamps avoid the somewhat critical and involved construction of the coaxial lamps and allow simple flashtube replacement. The linear flashlamps used for dye laser pumping were also originally developed for flash photolysis applications. These lamps have expansion chambers at each end to allow the shock wave to pass the electrodes and dissipate. As a result the tubes tend to be self-cleaning. Much of the material ablated from the lamp walls or eroded from the lamp electrodes is swept past the electrodes and accumulates in the ballast chambers. Consequently, lamp lifetime is somewhat superior to the coaxial devices. Linear flashtubes capable of withstanding a discharge energy of up to 200 joules in a 2 μsec pulse or up to 2000 joules in a 20 μsec pulse are commercially available. Fired at about 1/3 of their explosion energy these tubes give a useful lifetime in the range of 10,000 to 50,000 shots. Nevertheless, using commercial linear flashlamps as the pumping source Loth and Meyer (Ref. 15) have achieved a 1 watt average output from the rhodamine 6G dye laser. Schmidt (Ref. 16) similarly has obtained nearly 3.5 watts.

While both the coaxial and linear flashlamps can give efficient dye laser operation on a single pulse basis, neither is particularly well suited for fast repetition rate, high power operation. Moreover, the useful lamp lifetime is relatively short. The purpose of the present paper is to present data on a novel flashlamp utilizing a vortex gas flow field to positionally stabilize the arc in the center of the lamp. Since the arc does not touch the lamp wall, there is no erosion of the quartz jacket. Any material eroded from the lamp electrodes is carried away by the gas flow. Consequently, the useful lamp lifetime is extremely long. At 200 joules per pulse in a 2 μsec pulse the lifetime to half light output is in excess of 200,000 shots, and is limited primarily by the formation of color centers in the quartz lamp envelope. As a result of the fast gas flow and the relatively high gas pressure, the lamp is well suited for high repetition rate operation. Using this lamp as a source for pumping the dye, 10 watts of average output has been obtained from rhodamine 6G. This represents an average flashlamp input of 4 Kw, the limit available from the present power supply. Ultimately, much higher outputs should be possible with this type of device.

In Section II of this paper the so-called "short arc flashlamp" is described. The vortex stabilized lamp belongs to this generic category of flashlamp. The short arc flashlamp as generally described in the literature suffers from several shortcomings, which can be overcome by simply lengthening the arc. However, if the arc is lengthened to much over a centimeter some means must be provided to assure positional stability of the arc in the lamp. Vortex flow stabilization of pulsed

29

discharges is discussed in Section III. Section IV of this paper discusses a 250 joule vortex stabilized flashlamp. Finally Section V summarizes the paper and indicates possible future developments.

II. Short Arc Flashlamps

As mentioned in the introduction the short arc flashlamp is essentially a spark gap with a transparent enclosing wall. Such lamps have been investigated by a number of researchers (Ref. 17-21). An excellent summary of much of this work is given in a recent volume by F. B. A. Frungel (Ref. 21).

Short arc flashlamps offer good performance in terms of light output. For such lamps Glaser (Ref. 17) has reported electrical to optical output efficiencies of up to 15% in the spectral range from 2500 Å to 9000 Å. Frungel (Ref. 21) has reported up to 28% optical efficiency with nearly a third of the total emission occurring in the visible region. These efficiencies compare quite favorably with those of the linear or coaxial flashlamps used for dye laser pumping. For example, the measured optical efficiency of the linear lamps devised by Ferrar (Ref. 6) is approximately 20% over the region from 2000 Å to 6000 Å, with about 1/4 in the visible.

In regard to efficiency in short arc flashlamps, the most important parameters are the fill gas, the gas pressure, the arc length, the pulse duration and the input energy. The most commonly used fill gases are nitrogen, oxygen, hydrogen, carbon dioxide, argon, krypton and xenon. Of these gases, the most efficient by far are the rare gases, argon, krypton and xenon (Ref. 17, 19, 21). The efficiencies among these increase with the atomic weight. Various mixtures of the rare gases with small amount of nitrogen, hydrogen or carbon dioxide are often used either to quench the afterglow or to improve the voltage hold off properties. These gas mixtures are also quite efficient, when the rare gas constitutes the bulk of the mixture (Ref. 21).

The light output and efficiency of short arc flashlamps are found to increase with increasing arc length and with pressure (Ref. 17, 19, 21). The color temperature and efficiency also depend on the pulse duration and on the energy discharged. When the arc is first struck, the discharge occurs in a very narrow channel, which then expands at a rate dependent among other things on the energy discharged (Ref. 19). With a short duration discharge, the arc channel can expand very little. As a result of the very high energy density dissipated in the discharge, the arc temperature and the effective radiating color temperature are very high. The author has demonstrated flash durations as short as 0.05 μsec with input energies up to 10 joules (Ref. 22). However, the effective color temperature is in excess of 100,000 °K, and most of the radiated energy is short wavelength UV, which is absorbed by the quartz lamp envelope. Consequently, the useful optical efficiency is only about 1%. With microsecond pulse durations, the arc channel can expand

considerably and the color temperature is lower, generally in the range from 25,000 $^\circ$K to 75,000 $^\circ$K. The efficiencies are also higher, from 5 to 30% as discussed above. With still longer pulse durations, the arc can expand further, the color temperature is still lower, and the efficiency, higher. Discharging 1000 joules through a short arc flashlamp in a 200 μsec pulse, Frungel and Roder (Ref. 21) have obtained optical efficiencies of up to 60 percent.

The short arc flashlamp can be used to an advantage for fast repetition rate operation. In sealed-off or non-flowing flashlamps, the repetition rate is limited by the accumulation of ionized products in the discharge region with a subsequent decrease in firing voltage. Increasing the firing energy aggravates the problem. Ultimately, the lamp ceases to pulse and operates dc. At a cost of increased circuit inductance, and increased complexity, the problem can be alleviated by the use of a series switch, such as a thyratron or a spark gap. Alternatively, there are two approaches that one may take to increase the maximum repetition rate at which the flashlamp, itself, will operate. One approach is to attempt to accelerate ion recombination. Increasing the pressure is one effective means of accomplishing this goal. In this regard, it is worth noting that short arc flashlamps typically operate at fill pressures of from 1 to 20 atmospheres, and consequently, are capable of much higher frequency operation than the low pressure coaxial and linear flashlamps.

Another approach to high repetition rate operation is to remove the ions from the arc region in the time between successive firings. This is done by flowing the gas rapidly through the lamp. The maximum firing rate is determined, then, by the gas exchange rate. Frungel (Ref. 21) has succeeded in operating a fast flow lamp at 3000 pps with a discharge energy of 3 joules per pulse. At a reduced firing energy and with a sonic exit flow velocity operation at up to 50,000 pps is possible with this device. In practical applications, both approaches, high pressure and fast gas flow are useful.

One problem encountered in the short arc flashlamps is that the relatively low arc impedance is difficult to match with practical driving circuits. The result is extended ringing of the driving circuit and a loss of peak light output. This problem can be corrected by lengthening the arc in the lamp, provided that the positional stability of the arc can be maintained. As noted above lengthening the arc also increases the total light output and efficiency of the short arc flashlamp.

Empirically, the resistivity, ρ, of a spark discharge after the initial breakdown avalanche is found to be inversely proportional to the square root of the field strength (Ref. 19). Very roughly, then,

$$\rho \propto \sqrt{\ell/V} \qquad (2.1)$$

31

where ℓ is the gap separation and V the voltage. On the other hand, the radius, r_a, of the highly conducting arc channel is approximately proportional to the fourth root of the energy deposition per unit length (Ref. 19); that is,

$$r_a \propto \left(\frac{E}{\ell}\right)^{\frac{1}{4}} \tag{2.2}$$

where E is the total energy discharged. Consequently, the total arc resistance, R_a, is

$$R_a = \frac{\rho \ell}{\pi r_a^2} \propto \ell^2 \tag{2.3}$$

Although (2.3) cannot be regarded as quantitative, this result does underscore the desirability of a long arc for purpose of matching the lamp to the discharge circuit and, thus, maximizing lamp peak power and efficiency. However, with the longer arcs ($\ell \geq 2$ cm), arc stability becomes a severe problem. In any case, whether long or short, to be used effectively for laser pumping the lamp arc must be positionally stable.

III. Vortex Stabilization

The use of a gas vortex flow field for the stabilization of D. C. arc discharges is well known (Ref. 23-25). Two mechanisms operate to stabilize the arc along the axis of the vortex.

The inflow of cooler gases from the periphery of the lamp results in a radial temperature gradient with a maximum temperature on the vortex axis. In addition, the centrifugal forces arising from the swirling motion of the gas produces a radial pressure gradient with a pressure minimum along the axis. As result of the density and temperature dependence of the ionization processes both mechanisms contribute toward stabilizing the arc.

As generally operated the pressure gradient in D. C. vortex stabilized arc lamps is negligible (Ref. 23). Since the temperature gradient is not formed until after the arc is struck, care must be exercised in initiating the discharge. Generally, the arc is drawn; that is, the electrodes are pressed together, the arc is struck and the electrodes are then drawn apart. Such a procedure is not practical for a pulsed discharge, except possibly for high repetition rate operation (Ref. 27). However, the vortex flow can be arranged to produce a substantial

pressure gradient and this pressure gradient can be used to stabilize a pulsed discharge, even for single pulse operation.

The flow geometry used is shown in Fig. A-1. The gas is introduced into the lamp through a ring of jets located near the lamp wall at one of the electrodes, in this case the cathode. The jets inject the gas tangentially and with an axial pitch angle, θ. The gas passes along the length of the lamp and exits through a hole of radius, r_e, in the opposing electrode. The radius of the quartz tube confining the flow is r_o.

A considerable amount of analysis (Ref. 28) has been carried out on vortex flows such as shown in Fig. A-1. However, if end wall effects are neglected a relatively simple model can be used (Ref. 29). The variable describing the flow are the pressure, P, the density, ρ, and the radial, azimulthal and axial components of the flow velocity, u_r, u_φ, and u_z respectively. It is assumed that u_r, u_φ, ρ and P depend only on r, that is

$$\frac{dP}{dr} \gg \frac{dP}{dz}, \; \frac{dP}{d\varphi}, \; \text{etc.}$$

In the free flow region, $r_e \leq r \leq r_o$, the flow is essentially inviscid. Conservation of angular momentum gives:

$$u_\varphi (r) = \frac{r_o}{r} \; u_\varphi (r_o) \; ; \; r_e \leq r \leq r_o \qquad (3.1)$$

where $u_\varphi (r_o)$ is the tangential injection velocity at the wall. On the other hand, in the viscous core region, $0 \leq r \leq r_e$, the aximuthal velocity component must decrease uniformly to zero at the center. Using a straight line approximation:

$$u_\varphi (r) = \frac{r_o r}{r_e^2} \; u_\varphi (r_o) \; ; \; 0 \leq r \leq r_e \qquad (3.2)$$

33

The pressure is related to the azimuthal flow velocity as

$$\frac{dP}{dr} = \rho \ \frac{u_\varphi^{\ 2}}{r} \tag{3.3}$$

Further,

$$\rho = \frac{M}{RT} \ P \tag{3.4}$$

where M is the molecular weight of the flow gas, R is the gas constant and T is the temperature, here assumed to be uniform throughout the volume. Finally, from these results the pressure can be determined

$$P\ (r) = P(r_o) \ \exp \left\{ -\frac{1}{2} \ \frac{M}{RT} \ u_\varphi^{\ 2} (r_o) \ \left[\frac{r_o^{\ 2}}{r^2} \ -1 \right] \right\}$$
$$r_e \leq r \leq r_o \tag{3.5a}$$

$$P\ (r) = P(r_o) \ \exp \left\{ -\frac{1}{2} \ \frac{M}{RT} \ u_\varphi^{\ 2} (r_o) \ \left[\frac{2r_o^{\ 2}}{r_e^{\ 2}} \ -1 \ + \ \frac{r_o^{\ 2} r^2}{r_e^{\ 4}} \right] \right\}$$
$$0 \leq r \leq r_e \tag{3.5b}$$

The pressure ratio is:

$$\frac{P\ (o)}{P\ (r_o)} = \exp \left\{ -\frac{1}{2} \ \frac{M}{RT} \ u_\varphi^{\ 2} (r_o) \ \left[\frac{2r_o^{\ 2}}{r_e^{\ 2}} \ -1 \right] \right\} \tag{3.6}$$

From (3.6) it can be seen that the most critical factor determining the magnitude of the pressure gradient is the initial tangential injection velocity, $u_\varphi(r_o)$. With $r_e \sim 1/5\ r_o$, the tangential injection velocity must be $u_\varphi(r_o) \gtrsim 10^3$ cm/sec in order to obtain a significant pressure gradient. If the ring of injection jets is approximated by an annulus of width, d, equal to the jet diameter, the $u_\varphi(r_o)$ can be estimated as

$$u_\varphi (r_o) \cong \frac{F \cos \theta}{2\pi\, r_o d\, P(r_o)} \tag{3.7}$$

Here F is the volumetric flow rate reduced to standard conditions, and $P(r_o)$ is expressed in atmospheres. With $r_o \sim 2$ cm, $d \sim 0.15$ cm and $\theta \sim 15o$, then for a significant pressure gradient

$$\frac{F}{P(r_o)} \gtrsim 0.6 \text{ liter/sec-atm} \tag{3.8}$$

As noted earlier this condition generally is not fulfilled in the high pressure vortex stabilized D. C. arc lamps.

Figure A-2 shows the actual pressure distribution in a lamp designed for pulsed operation. This flashlamp is described in more detail in the following section. In this case the flow rate is 5 ℓ/sec STP of argon and the wall pressure is 1.76 atm. The tangential injection velocity estimated from (3.7) is $u_\varphi (r_o) = 3 \times 10^3$ cm/sec. The solid curve in Fig. A-2 is the pressure distribution calculated from (3.5a) and (3.5b). The agreement with the experimental data is excellent, especially considering the approximations involved in the present model for the flow. It should be noted that the experimental pressure measurement was repeated at several positions axially between the electrodes, with essentially identical results.

It remains to be shown that a pressure distribution such as that in Fig. A-2 can stabilize the breakdown in a pulsed discharge. To this end Fig. A-3 shows two dimensional model for a vortex stabilized flashlamp in this case with a 3 cm arc length. The lower electrode is taken to have a potential, $\varphi = 1$, while the upper electrode is at ground potential, $\varphi = 0$. Ground returns are located adjacent to the lower electrode to minimize lamp inductance (see following section). The quartz tube, which is not shown in Fig. A-3 prevents breakdown between the ground returns and the lower electrode. The equipotential surfaces for this structure were determined by the use of a teledeltos paper model (Ref. 30). These equipotential curves are also shown in Fig. A-3.

From the equipotential surfaces (Fig. A-3) the electric field distribution can be determined everywhere within the lamp. The electric field distribution combined with pressure distribution data (Fig. A-2) can then be used to map the E/P ratio, where E is the electric field magnitude. It is convenient to plot E/P on the equipotential surfaces as a function of radius. This is shown in Fig. A-4 for the lamp with the 3 cm arc (Fig. A-3). The E/P ratio reaches a maximum at the axis for both electrodes (φ = 0.2, 0.4, 0.6, 0.8). Due to the strong dependence of the ionization avalanche in a collision dominated breakdown on the E/P ratio (Ref. 31), this is sufficient to assure that the discharge will occur on the axis.

Figure A-5 illustrates E/P for a lamp similar to that in Fig. A-3 but with a 6 cm arc length. Again the pressure distribution of Fig. A-2 was assumed. As in the case of the 3 cm arc length, the E/P ratio is at least a relative maximum on the axis and is an absolute maximum on axis at both electrodes. If the arc length is increased an additional 3 cm, this is no longer true. However, experimentally, the 6 cm arc length flashlamp is completely stable and entirely reliable.

IV. 250 Joule Vortex Stabilized Flashlamp

The construction of a high power vortex stabilized flashlamp with a 6 cm arc length is shown in Fig. A-6. The lower electrode, the lamps cathode, is connected to the high voltage terminal of a low inductance, 2 μf, 25 Kv capacitor (Tobe Deutschmann ESC-506). The flashlamp anode is supported by a ground return cage, which surrounds the 4 cm diameter 0.25 cm wall, fused quartz lamp envelope. The support cage for the upper electrode consists of six pairs of 1/8" diameter hollow brass tubes with each pair oriented radially and with the pairs arranged in a regular hexagon about the lamp envelope. The exiting gas flow is carried through these tubes. The electrodes are 1/2" diameter tungsten and are hemispheric in shape.

The gas flow enters the arc region through eight 0.060" diameter jets surrounding the lamp cathode. These jets are located about 10 cm below the cathode tip to allow the individual jet streams to diffuse. If this is not done, there is some tendency for the arc to strike along the individual jet streams. Otherwise, the construction of the vortex nozzle is not critical. The gas leaves the arc region through a 1/4" diameter hole in the anode. As mentioned in the previous section the fill gas is argon and flow rate is 5 ℓ/sec STP. The pressure distribution is given in Fig. A-2 and the wall pressure is 1.76 atm. Above 8 Kv a variable (0-10%) amount of CO_2 is added to the gas stream to increase the voltage holdoff of the argon.

Fig. A-6b shows several successive firings of the lamp. Within the measurement accuracy ($\sim$ 20% of the arc diameter) the arc always restrikes down the same channel. At reduced gas flow rates, the arc will become bowed and the arc channel will be non-reproducible. If the flow rate is decreased sufficiently, the arc will strike

from the center electrode to the quartz envelope near one of the tube pairs, where the electric fields are high, and up the quartz envelope to the upper electrode. This will inevitably shatter the quartz tube. Even at full flow there is some tendency at high repetition rates for the arc to strike along this path. This difficulty can be eliminated by insulating the center electrode with an alumina sleeve (see Fig. A-6a) and most importantly, by applying a negative voltage to the center electrode eliminates positive corona effects (Ref. 32).

The flashlamp can be externally triggered by the use of a third electrode. This trigger electrode can be mounted either coaxially within the exit orifice in the upper main electrode or coaxially in a second exit orifice in the lower main electrode. Effective triggering can be achieved with the center electrode. Triggering at a positive electrode requires less energy in the trigger discharge for reliable triggering than does negative electrode triggering (0.05J. vs. 0.5J.). However, negative electrode triggering gives a substantially reduced delay and jitter than does positive electrode triggering even if the latter is operated at the same discharge energy (see Fig. A-7). This difference in behavior has also been observed in the more usual sealed-off short arc flashlamps (Ref. 21). In the present version of the device the trigger discharge is located in the lower main electrode which is the lamp cathode. The delay and jitter are of the order of 2 μsec.

Fig. A-8 shows voltage and current measurements made at the capacitor during the flash discharge at 100 joules input. The total circuit inductance as determined from the current and voltage ringing frequency is 155 nanohenries. Of this approximately 80 nh is due to a single turn external series "inductor" added to the circuit for the purpose of slowing the electrical risetime and, thus, decreasing the shock wave intensity within the lamp. With the addition of this series inductance the explosion limit for the lamp is increased from approximately 140 joules to over 300 joules, and the lamp may be reliably operated to 250 joules at high repetition rates without fear of breakage. In terms of light output the series loop does lengthen the flash risetime by 30 to 40 percent but the peak light output is unaffected and the flash duration is only slightly increased.

In Fig. A-8c the peak electrical power delivered to the lamp circuit is seen to be approximately 50 Mw. As in the case of the coaxial lamps the light output lags considerably behind the power input (Ref. 10). The lamp impedance is shown in Fig. A-8d. The impedance is purely resistive, where $dI/dt = 0$. Comparing Fig. A-8b and Fig. A-8d shows the lamp resistance to be nearly constant at approximately 0.2 Ω during the discharge.

The flash output from the lamp is shown in more detail in the oscilloscope traces shown in Fig. A-9. These measurements were made with an S-5 surface vacuum photodiode. At an input of 36 joules as well damped, symmetrical flash output was obtained. The risetime of the optical output is approximately 0.8 μsec and the flash duration (FWHM) is 1.6 μsec. Ninety percent of the radiated energy appears

within 2.2 μsec after initiation of the discharge. At 200 joules per pulse the flash is asymmetric with a pronounced tail. The flash risetime has decreased to 0.6 μsec, but the flash duration is increased to 1.7 μsec. As a result of the slowly decaying tail, the time required to radiate 90% of the total optical output is increased to 3.2 μsec. It should be noted that each of the photographs in Fig. A-9 represents 10 firings of the lamp. The 10 outputs superimpose within the trace width in the photographs.

Calorimetric measurements were also made on the lamp output. For these measurements a cylindrical calorimeter was constructed to fit over the lamp and intercept nearly all of the radiated output from the lamp. The calorimeter consisted of two concentrically mounted thermally isolated copper tubes with the inner tube serving as the calorimeter target and the outer tube, as the reference. The inside surface of the target cylinder was roughened by sandblasting and darkened by a chemical blackening agent. For purposes of the measurement the blackened surface was assumed to be completely absorbing. The calorimeter was calibrated by discharging a known energy through a fine filament wrapped around the inner cylinder and measuring the subsequent temperature rise.

The results of the calorimetric measurements are shown in Fig. A-10. The output efficiency, that is the ratio of radiated optical output energy to stored electrical energy, reaches a maximum of 17% at an input of 60 joules. At higher energies the efficiency decreases gradually to about 13% at 225 joules.

Figure A-11 shows the spectral distribution of the radiated lamp output. These data represent vacuum photodiode (RCA 935) measurements taken through a 1 meter spectrometer (Jarrell-Ash model 75-152). The relative spectral sensitivity of the photodiode-spectrometer combination was calibrated using a standard tungsten source. The spectral distribution is roughly the same at 100 and 200 joule inputs. In both cases the effective radiating color temperature is approximately 70,000 $^{\circ}$K.

While the 70,000 $^{\circ}$K color temperature is extremely high from the point of view of more conventional light sources, such color temperatures are not uncommon for spark sources (Ref. 21). Moreover, assuming the lamp radiates according to the Stefan-Boltzman law and knowing the flash duration, the radiating surface area, and the temperature, the total lamp output through the quartz can be determined. At 70,000 $^{\circ}$K., a perfect black body will radiate 1.4×10^8 watts/square cm. Approximately 4.9% of this radiation will pass through the quartz ($\lambda > 1800$ Å). At a 200 joule input, the flash duration (FWHM) is 1.7 μsec and the luminous arc diameter, determined photographically (Fig. A-12) is approximately 0.7 cm. Using these data, the calculated optical output is 27 joules, agreeing exactly with the measured result (Fig. A-10). While the excellent agreement is likely fortuitous, the fact that the measured and calculated output are roughly equal does lend confirmation to the color temperature measurement.

It might be observed that in contrast to the more usual wall stabilized flashlamps, the luminous arc diameter in the vortex stabilized flashlamp will vary with input energy. In fact, since the lamp efficiency (Fig. A-10) and color temperature (Fig. A-11) are roughly constant with input energy, E, the luminous arc diameter would be expected to vary as $\sqrt{E}$ according to the considerations above. Such a dependence is consistent with the results of Fig. A-12.

Life testing has been carried out on this lamp. At 200 joules per pulse the lamp life to half light output is of the order of several hundred thousand shots. The limitation to lamp life at this point is the formation of color centers in the quartz envelope due to intense ultraviolet irradiation. These color centers can be removed by re-annealing the quartz. Alternately, the problem could be corrected by the use of a suprasil grade fused silica envelope, rather than the commercial grade quartz in use at present.

Finally a significant advantage of the vortex stabilized flashlamp is its ability to operate at a relatively high pulse repetition rate.

V. Conclusions

The vortex stabilized flashlamp has been demonstrated to be an efficient and reliable light source. It is particularly well suited for applications requiring high average power and a long operational lifetime. With a fast driving circuit the vortex stabilized flashlamp is an ideal source for dye laser pumping. With a more conventional discharge circuit, the lamp should also be well suited for pumping other optically pumped lasers not requiring a fast risetime pumping pulse.

In terms of future developments, vortex stabilized D. C. arc lamps are commercially available at up to 150 Kw (Ref. 24). The present vortex stabilized flashlamp has been operated to a maximum input of about 4 Kw. Much higher power operation should be possible. The major impediment to very high power operation would most likely be the accumulation of ionized species in the arc region. As discussed in Section II several approaches can be used to circumvent this problem.

Finally, in all of the work described here argon has been used as the fill gas. In terms of optimizing the flashlamp output, particularly in the visible region of the spectrum, xenon may be a better choice (Refs. 17, 21). In the case of the coaxial flashlamps xenon gives nearly an order of magnitude increase in dye laser efficiency over argon (Ref. 10). While such a large increase is not likely here, an improvement should still be possible. The only difficulty with xenon is its expense. Open cycle gas flow such as used here with the argon is not practical with xenon, but instead a closed cycle gas recirculation system must be developed. This has been done with some of the commercial D. C. arc lamps and it could be done with vortex stabilized flashlamp.

REFERENCES FOR APPENDIX I

1. Sorokin, P. P., J. R. Lankard, V. L. Moruzzi and E. C. Hammond:
    J. Chem. Phys., 48, 4726, (1968).

2. Sorokin, P. P., J. R. Lankard, E. C. Hammond and V. L. Moruzzi:
    IBM Res. Develop. 11, 130 (1967).

3. Tuccio, S. A.: Paper 1.2, 1971 IEEE/OSA Conference on Laser
    Engineering and Applications.

4. Pappalardo, P., H. Samelson and A. Lempicki: Appl. Phys. Letters,
    16, 267, (1970).

5. Marling, J. B., D. W. Gregg, and L. Wood: Appl. Phys. Letters,
    17, 527, (1970).

6. Ferrar, C. M.: Rev. Sci. Instr. 40 1436 (1969).

7. Schuler, C. J., C. T. Pike, and H. A. Miranda: to be published

8. Bradley, D. J.: Paper 1.1, 1971 IEEE/OSA Conference on Laser
    Engineering and Applications.

9. Anliker, P., M. Gallmann and H. Weber: Optics Communications, 5,
    137 (1972).

10. Furumoto, H. W. and H. T. Ceccon: Appl. Opt. 8, 1613, (1969).

11. Huth, B. G. and M. R. Kagan: IBM, J. Res. Develop, 15, 278, (1971).

12. Galaktionova, N. M., and A. A. Mak: Opt. Spektrosk. XVI, 153 (1964).

13. Claesson, S., and L. Lindqvist: Arkiv Kemi, 12, 1, (1957).

14. Furomoto, H. W., and H. L. Ceccon: IEEE J. Quantum Electronics,
    6, 262, (1970).

15. C. Loth and Y. H. Meyer, Appl. Optics 12, 123 (1973).

REFERENCES (CONT'D)

16. W. Schmidt, Laser 4, 47 (1970); Appl. Phys. Letters 20, 71 (1972).

17. Glaser, G.: Optik, 1, p. 33, (1950).

18. Kirsanov, V. P., V. A. Gavanin and I. S. Marshak: Opt. and Spectr., 13, p. 153 (1962).

19. Marshak, I. S.: Sov. Phys. Uspek. 5, p. 478 (1962).

20. Andreev, S. I., and M. P. Vanyukov: Sov. Phys. - Tech. Phys. 6, p. 700 (1962).

21. Frungel, F. B. A.: High Speed Pulse Technology, Vol. II, Academic Press, New York, (1965).

22. Mack, M. E.: Paper 1.5, 1971 IEEE/OSA Conference on Laser Engineering and Applications.

23. M. B. Zhitkova, V. M. Krivtsun, A. I. Portnyagin and A. A. Shokin, Sov. J. Quant. Elect. 1, 238 (1971).

24. W. W. Cann, Appl. Opt. 8, 1645 (1969).

25. J. E. Anderson, R. C. Eschenback and H. H. Troue, Appl. Opt. 4, 1435 (1965).

26. B. Vonnegut, C. B. Moore and C. K. Harris, J. Meterology 17, 468 (1960).

27. E. M. Wilkins and L. T. McConnell, J. Geophysical Research 73, 2559 (1968).

28. See for example, M. L. Rosenzweig, M. S. Lewellen and D. H. Ross, AIAA Journal 2, 2127 (1964); M. S. Lewellen, AIAA Journal 3, 91 (1965); O. L. Anderson, UARL Report R2494-1 (1961).

29. J. C. Hunsaker and B. G. Rightmire, Engineering Applications of Fluid Mechanics p. 76, McGraw Hill, N.Y. (1947).

REFERENCES (CONT'D)

30. D. Vitkovitch, _Field Analysis_, Chapt. 5, Van Nostrand London (1966).

31. See for example, A. von Engel, _Ionized Gases_, Chapt. 7 Oxford, London (1955).

32. L. B. Loeb, _Electrical Coronas_, University of California Press, Berkeley (1965).

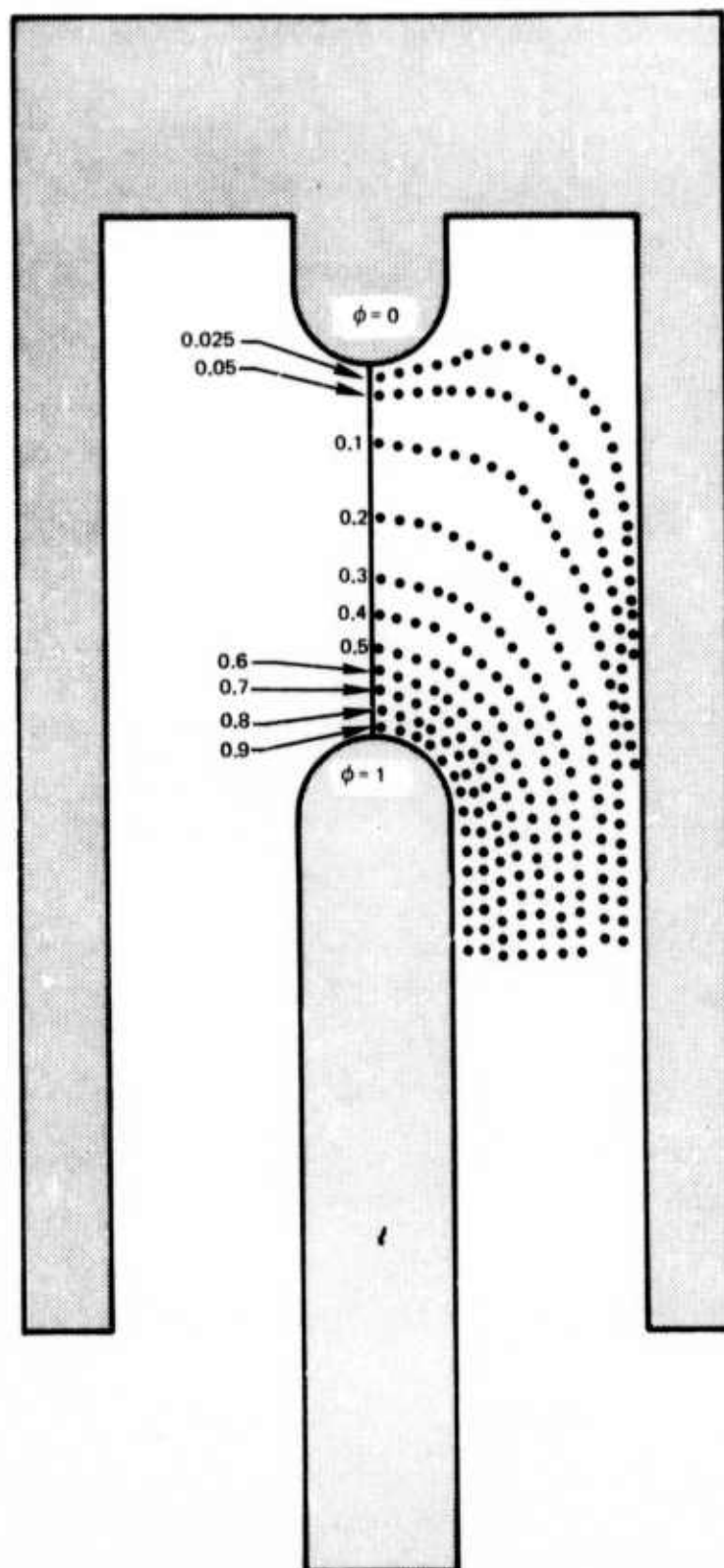33. M. E. Mack, Appl. Phys. Letters 19, 108 (1971).
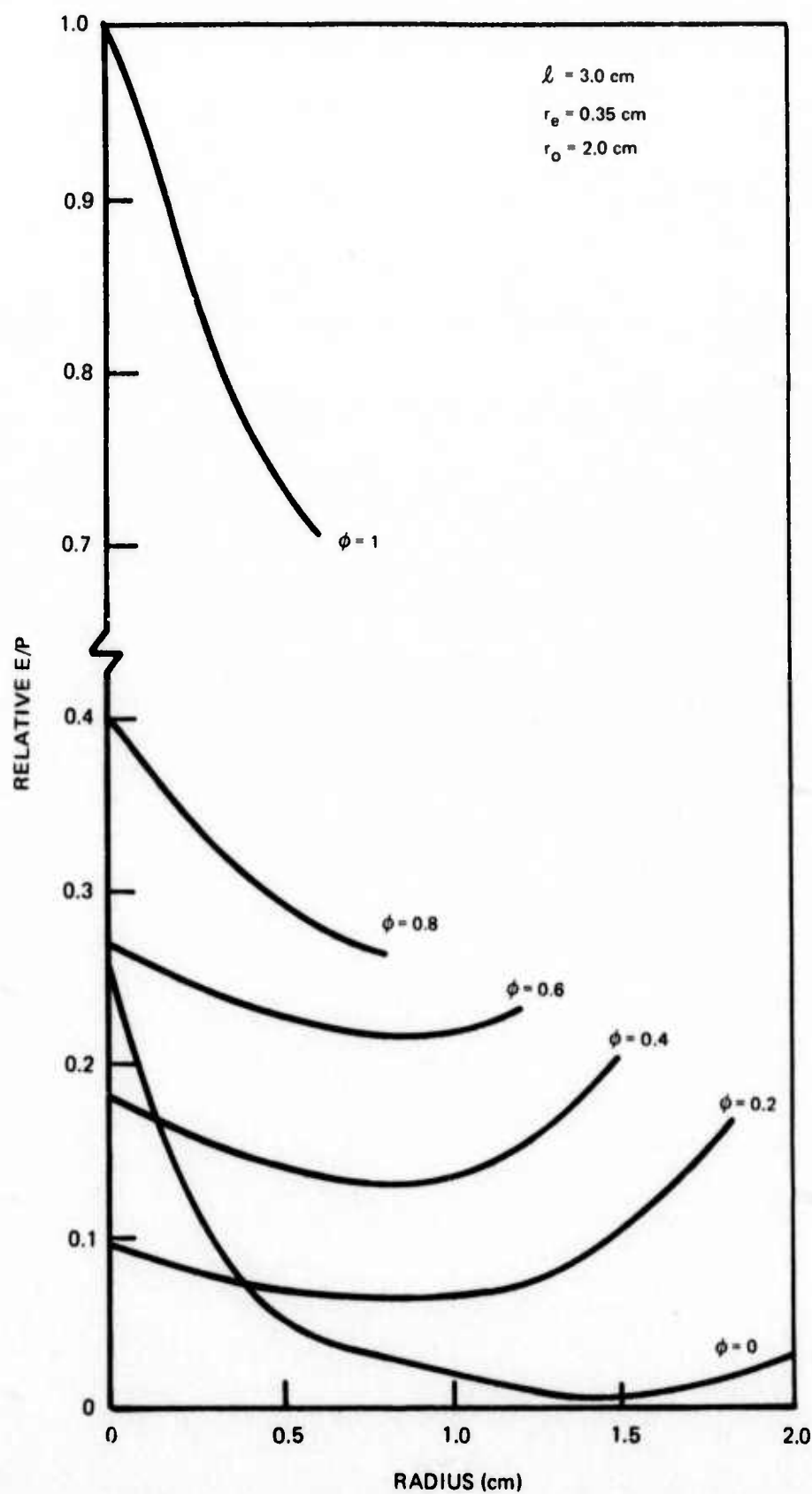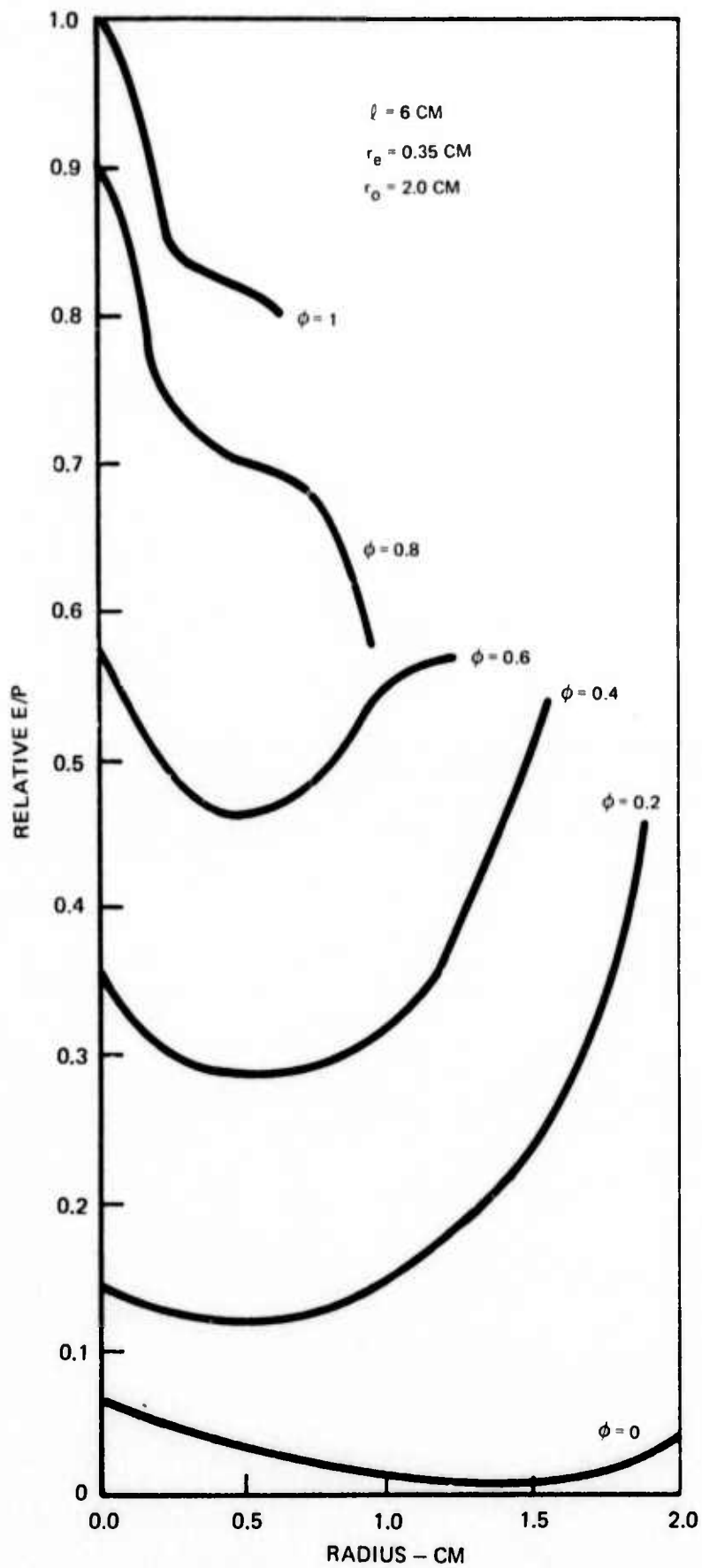
VORTEX FLOW SCHEME
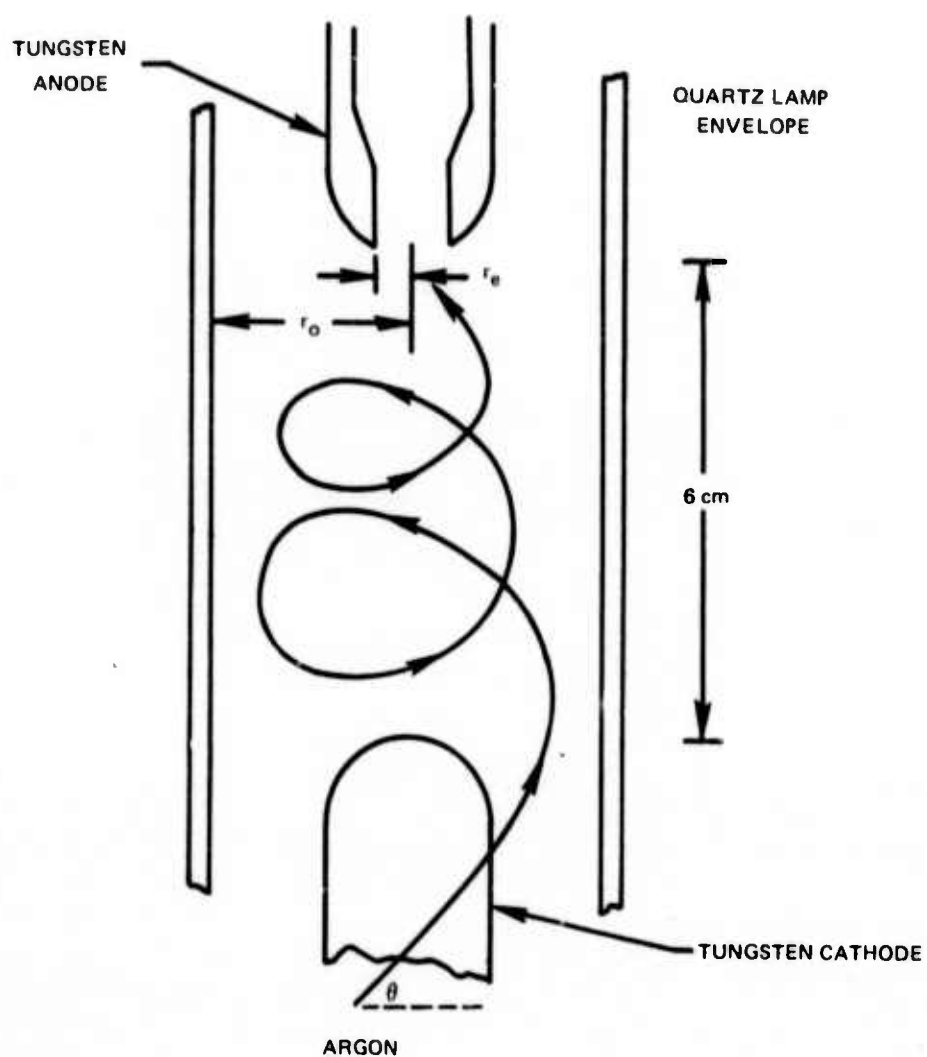
LAMP PRESSURE GRADIENT

$\ell = 6\ \text{CM}$

$r_e = 0.35$
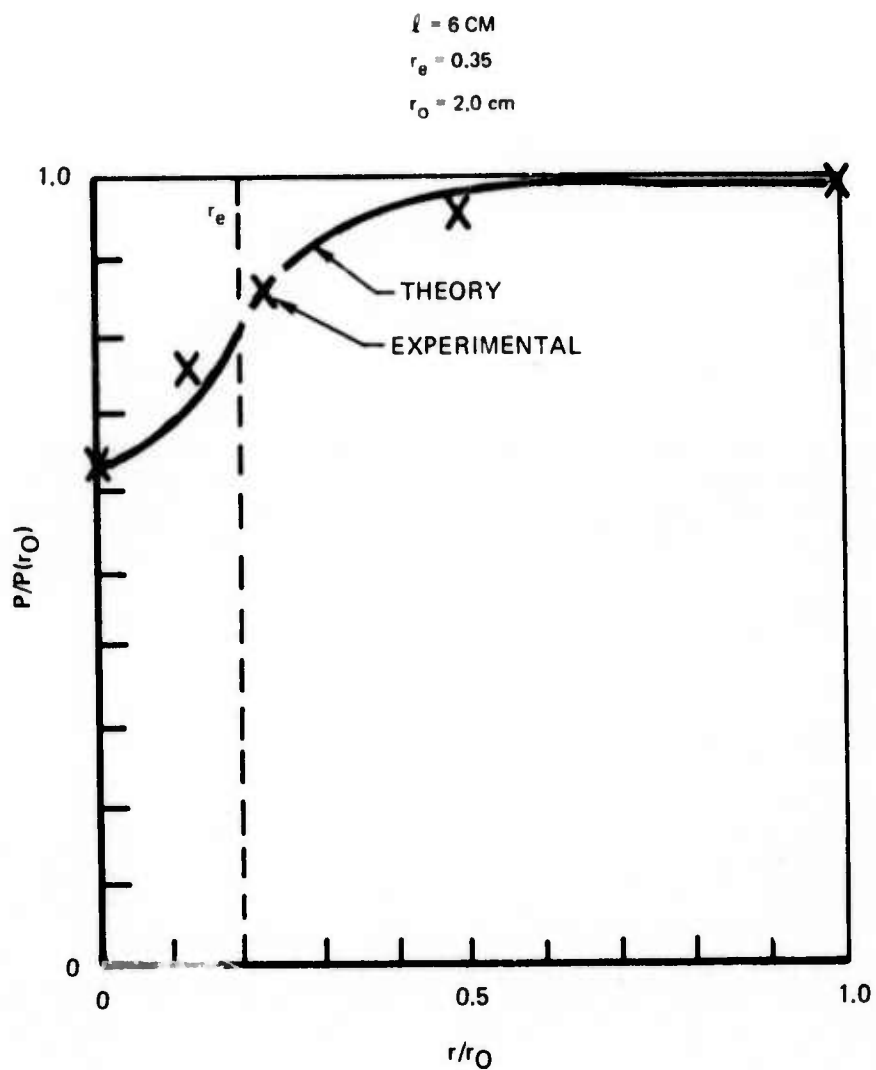
$r_0 = 2.0\ \text{cm}$

FLASHLAMP POTENTIAL DISTRIBUTION

E/P RATIO ON THE EQUIPOTENTIAL SURFACES

3 CM ARC

ℓ = 3.0 cm

r_e = 0.35 cm

r_o = 2.0 cm

RELATIVE E/P

ϕ = 1

ϕ = 0.8

ϕ = 0.6

ϕ = 0.4

ϕ = 0.2

ϕ = 0

RADIUS (cm)

46

E/P RATIO ON THE EQUIPOTENTIAL SURFACES
6 CM ARC

$\ell = 6$ CM

$r_e = 0.35$ CM

$r_o = 2.0$ CM

$\phi = 1$

$\phi = 0.8$

$\phi = 0.6$

$\phi = 0.4$

$\phi = 0.2$

$\phi = 0$

RELATIVE E/P

RADIUS – CM

250 JOULE VORTEX STABILIZED FLASHLAMP
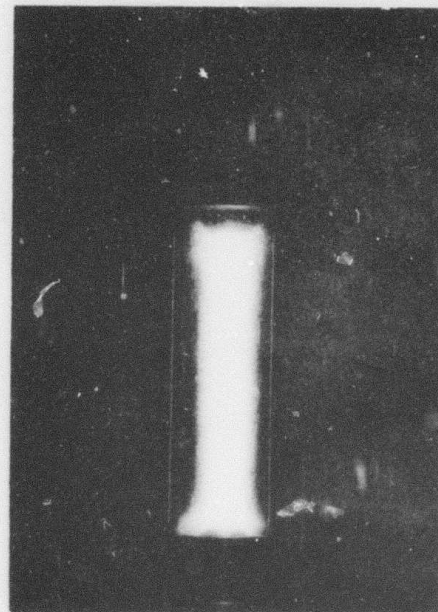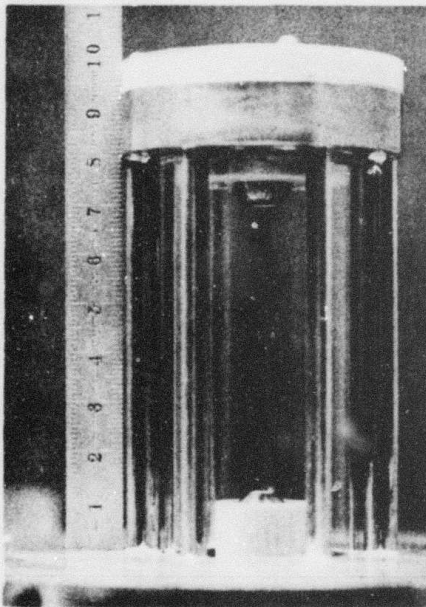
EXTERNAL TRIGGERING

NEGATIVE ELECTRODE TRIGGERING

2 μsec/cm

POSITIVE ELECTRODE TRIGGERING

CAPICITOR VOLTAGE
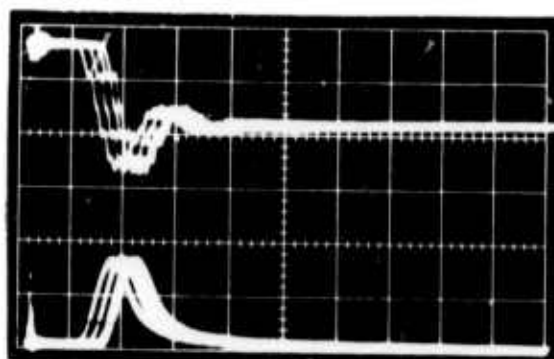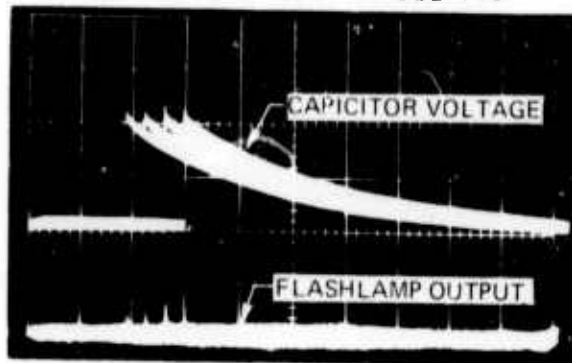
FLASHLAMP OUTPUT

0.5 msec/cm

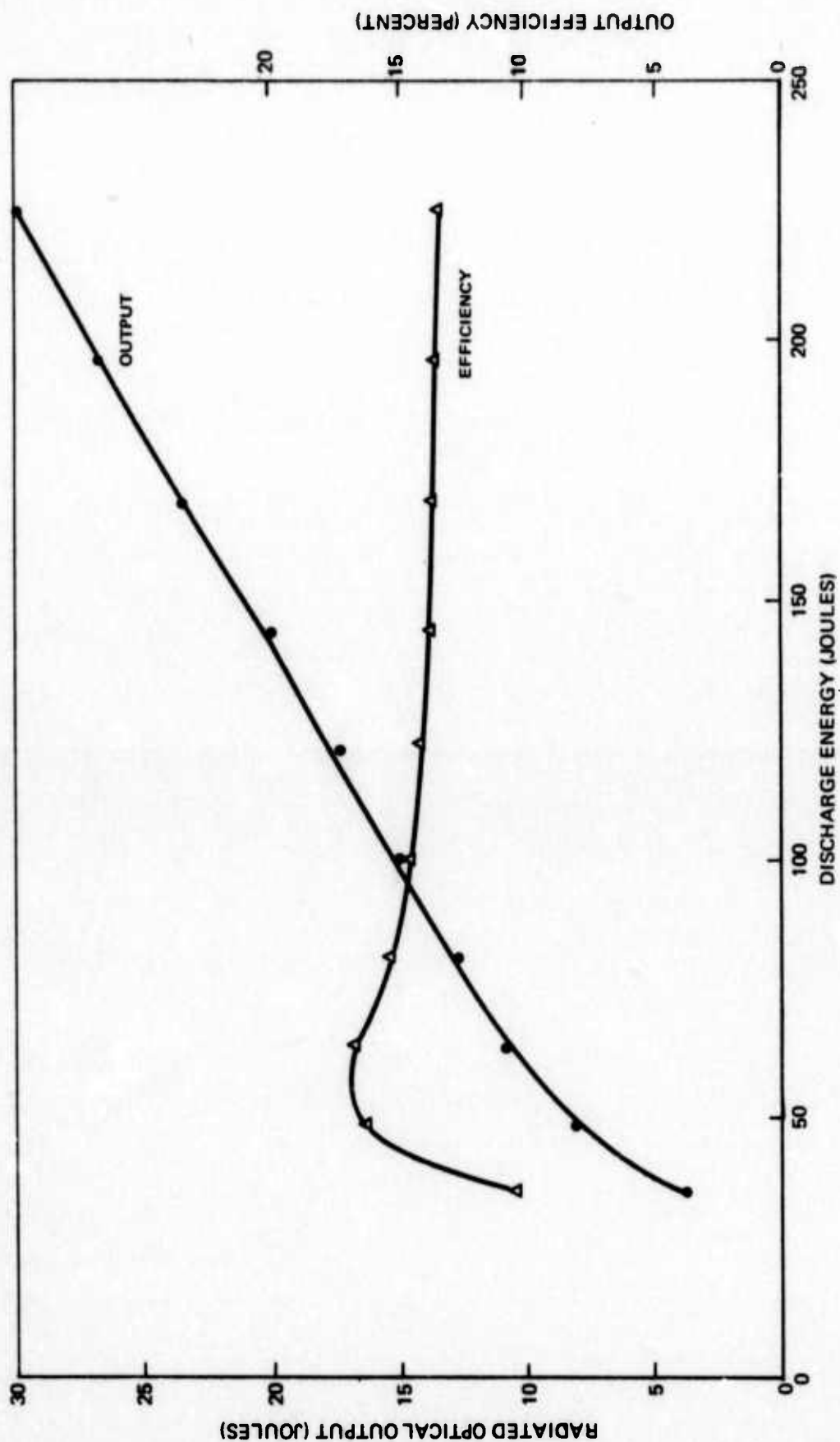## ELECTRICAL MEASUREMENTS
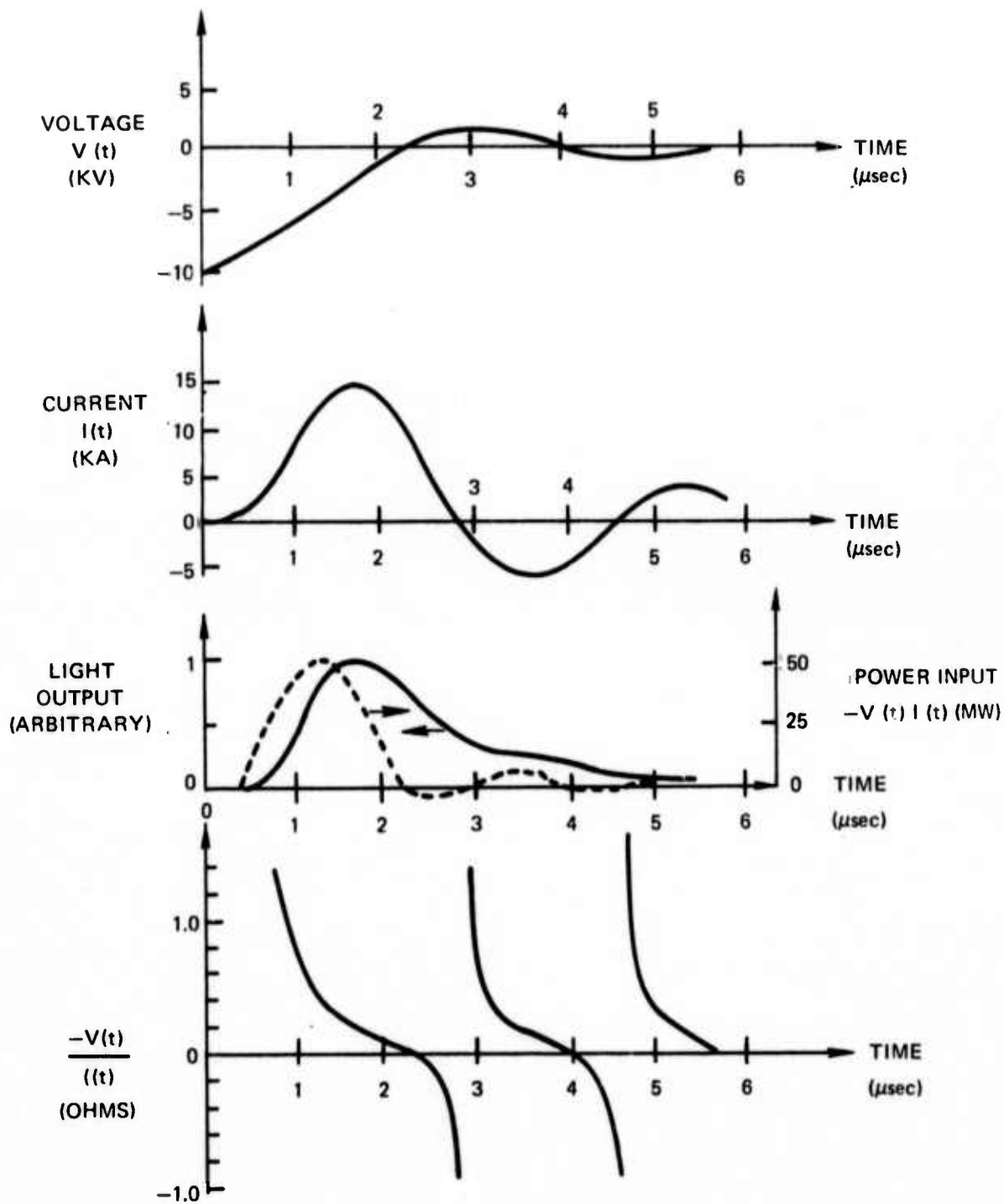
FLASHLAMP OUTPUT
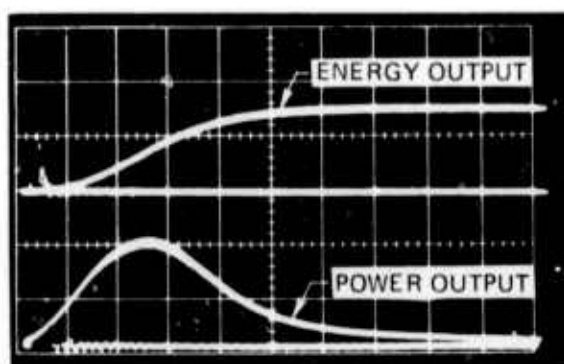
36 J — 10 SHOTS
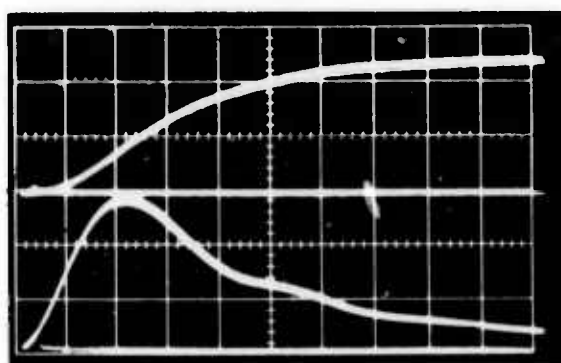
200 J — 10 SHOTS

0.5 μsec/cm
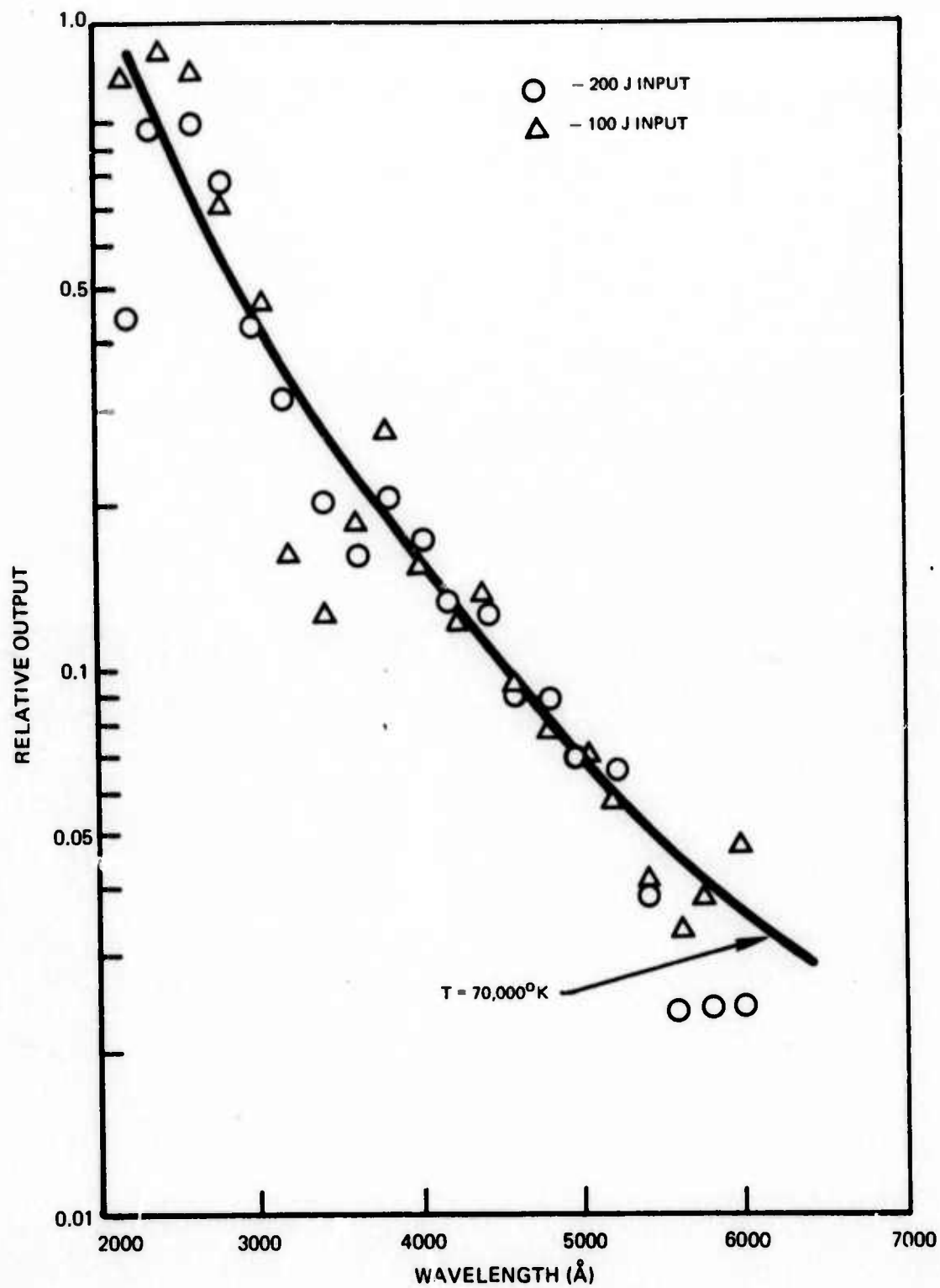
CALORIMETRIC OUTPUT MEASUREMENT

SPECTRAL DISTRIBUTION

APPARENT LUMINOUS ARC DIAMETER